UNIVERSIDADE BEIRA INTERIOR

Impact of High Frequency repetitive Magnetic Stimulation on Astrocytes Subjected to Ischemia

Susana Maria Alves Ferreira

Dissertação para obtenção do Grau de Mestre em

Ciências Biomédicas

(2º ciclo de estudos)

Orientadora: Professora Doutora Graça Maria Fernandes Baltazar

outubro de 2022

Declaração de Integridade

Eu, Susana Maria Alves Ferreira, que abaixo assino, estudante com o número de inscrição m10939 do mestrado em Ciências Biomédicas da Faculdade de Ciências da Saúde, declaro ter desenvolvido o presente trabalho e elaborado o presente texto em total consonância com o **Código de Integridades da Universidade da Beira Interior**.

Mais concretamente afirmo não ter incorrido em qualquer das variedades de Fraude Académica, e que aqui declaro conhecer, que em particular atendi à exigida referenciação de frases, extratos, imagens e outras formas de trabalho intelectual, e assumindo assim na íntegra as responsabilidades da autoria.

Universidade da Beira Interior, Covilhã 27/10/2022

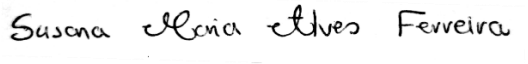

This work was developed within the scope of the CICS-UBI projects UIDP/Multi/00709/2019, UIDB/Multi/00709/2019, UIDP/00709/2020, and UIDB/00709/2020, financed by national funds through the Portuguese Foundation for Science and Technology/MCTES, and by funds to the PPBI-Portuguese Platform of Bio Imaging through the Project POCI-01-0145-FEDER-022122.

I would like to thank Cláudio Maia (CICS-UBI) for the help with the PCR analysis and the CICS-UBI microscopy Unit for the technical support.

Agradecimentos

À minha orientadora, Professora Doutora Graça Baltazar, pela confiança que depositou em mim para a realização deste projeto e pela sua incansável ajuda. O meu sincero obrigada pela oportunidade e pelos conhecimentos transmitidos, mas também pela amizade e apoio nos percalços ao longo deste trabalho. Agradeço em especial a liberdade que nos dá para termos novas ideias e testarmos novas técnicas que ajudam a enriquecer o nosso projeto. O seu rigor e a sua exigência inspiram-me e ajudaram-me a crescer, não só como cientista, mas também como pessoa.

À Professora Doutora Maria da Assunção Vaz Patto e ao Professor Doutor Nuno Pinto pela colaboração e disponibilidade ao longo deste ano, a vossa ajuda foi essencial para a realização deste projeto!

Ao Professor Doutor Claúdio Roque, obrigada por toda a ajuda inicial e adaptação ao mundo da investigação!

Aos meus colegas e amigos, Diana Costa, Beatriz Almeida, Mafalda Proença, Tânia Silva e Diogo Almeida, muito obrigada por todos os momentos ao longo deste ano. Juntos, os desafios da investigação tornaram-se mais fáceis de superar. Um especial obrigada à Mafalda Dinis por estar sempre disposta a ajudar!

À Inês Serrenho, um agradecimento muito especial! Obrigada por toda a ajuda ao longo deste ano, por todos os conhecimentos transmitidos, por tudo o me ensinaste sem teres qualquer obrigação! Este ano foi infinitamente mais fácil com a tua ajuda! Pelas horas que passaste comigo no biotério, no laboratório, na salinha. Por todos os pedacinhos de tempo que arranjaste para me ajudar, mesmo estando sempre tão ocupada. Obrigada pelo companheirismo, pelos dias que saímos tardíssimo da faculdade e pela motivação para nunca desistir mesmo quando nada estava a dar certo. Mas acima de tudo, obrigada pela amizade! És para mim uma inspiração, tanto profissional como pessoal! Espero sinceramente que consigas alcançar tudo aquilo a que te prepuseres e que a vida te sorria sempre!

À minha família, a quem dedico este trabalho, obrigada pelo apoio e pelos sacrifícios que fazem para eu poder estar aqui. Sem vocês nunca teria chegado até aqui!

Ao Tomás, obrigada pelo amor, carinho e cumplicidade ao longo de todos estes anos! Obrigada pelo apoio, ajuda e compreensão. Contigo, a vida é tão mais fácil e feliz! Obrigada pela paciência e por sempre acreditares que sou capaz!

Resumo

O acidente vascular cerebral isquémico (IS, do inglês *ischemic stroke*) é causado pela redução ou bloqueio do fluxo sanguíneo para o cérebro e é a terceira causa de morte mais comum em Portugal. A estimulação magnética transcraniana repetitiva de alta frequência (HF-rTMS, do inglês *high-frequency repetitive transcranial magnetic stimulation*) tem sido considerada uma estratégia terapêutica promissora para o IS, visto ter a capacidade de melhorar as sequelas mais frequentes causadas pela isquemia cerebral. As melhorias observadas têm sido associadas a alterações neuronais. Contudo, levantou-se a hipótese de esta técnica modular as astrócitos, potenciando as suas capacidades neuroprotetoras. Com o presente trabalho, pretendemos esclarecer quais os mecanismos desencadeados pela estimulação magnética repetitiva de alta frequência (HF-rMS, do inglês *high-frequency repetitive magnetic stimulation*) em astrócitos que contribuem para os seus efeitos neuroprotetores.

Foi realizado um modelo *in vitro* de isquemia com culturas de astrócitos e culturas mistas de neurónios e astrócitos corticais sujeitas a privação de oxigénio e glicose (OGD, do inglês *oxygen and glucose deprivation*). A neuroprotecção promovida pela HF-rMS foi avaliada através da análise de marcadores de atividade neuronal e da análise morfométrica dos neurónios. Os níveis de fatores de crescimento no meio condicionado de astrócitos (CM, do inglês *conditioned medium*) foram avaliados através de um Array de fatores de crescimento e a expressão do fator neurotrófico derivado da glia (GDNF) foi analisada por RT-PCR e por Western Blot.

Os nossos resultados mostram que a modulação dos astrócitos pela HF-rMS promove a recuperação neuronal após um insulto isquémico. Esta modulação ajuda a manter o número e o comprimento das neurites e aumenta o número de neurónios que expressam c-Fos. A avaliação dos níveis dos transportadores de glutamato EAAT1 e EAAT2 nos astrócitos mostrou que o EAAT2 não foi afetado pela HF-rMS, contudo, o EAAT1 aumentou em culturas sujeitas a OGD e HF-rMS, sugerindo que a neuroprotecção promovida pela HF-rMS pode envolver uma redução da excitotoxicidade. Além disso, a análise do CM de astrócitos mostrou que a HF-rMS estimulou a libertação de vários fatores tróficos pelos astrócitos, nomeadamente o GDNF. A neutralização do GDNF presente no CM de astrócitos impediu a recuperação do número de neurites e do seu comprimento induzido pela HF-rMS e diminuiu o número de neurónios c-Fos$^+$, indicando que este fator neurotrófico desempenha um papel crucial na recuperação neuronal induzida pela HF-rMS.

Em conjunto os resultados obtidos mostraram que a modulação de astrócitos pela HF-rMS é capaz de recuperar os neurónios lesionados pela isquemia, diminuindo a excitotoxicidade e promovendo a neuroprotecção através da libertação de GDNF pelos astrócitos. Esta observação sugere que, ao modular os astrócitos, a HF-rMS pode ser utilizada para promover a neuroprotecção em outras lesões cerebrais.

Palavras-chave

Acidente vascular cerebral isquémico; estimulação magnética repetitiva de alta frequência; astrócitos; neuroprotecção; GDNF.

Resumo Alargado

O IS é causado pela redução ou bloqueio do fluxo sanguíneo para o cérebro atingindo, anualmente, cerca de 15 milhões de pessoas, e corresponde à terceira causa de morte mais comum em Portugal.

Apesar da alta incidência, não existem terapias eficazes em promover a recuperação dos tecidos cerebrais lesionados pela isquemia. As terapias existentes baseiam-se na reposição do fluxo sanguíneo para limitar a extensão da lesão, ou, mais tarde, na redução de défices específicos causados pelo IS através de fisioterapia e/ou terapia da fala. A HF-rMS é uma técnica de estimulação não invasiva e indolor, que está indicada para o tratamento pós-agudo da isquemia. Esta técnica é usada na clínica com resultados favoráveis ao nível da função motora, afasia, heminegligência, disfagia e défices cognitivos, mas os dados relativos aos efeitos celulares causados pela HF-rMS centram-se principalmente nos efeitos neuronais.

Na HF-rMS uma corrente elétrica passa através de uma bobina colocada sobre o escalpe, fazendo gerar campos magnéticos que atravessam o crânio e modificam a atividade das células cerebrais. Quanto mais alta a intensidade, mais profundamente os campos magnéticos conseguem penetrar o cérebro, modulando a atividade de estruturas mais profundas. O campo magnético induz uma corrente elétrica no cérebro que vai induzir um fluxo de iões alterando a carga elétrica nas membranas celulares e levando à despolarização ou hiperpolarização neuronal. Nos últimos anos, a HF-rMS tornou-se uma técnica promissora para a recuperação das funções cerebrais e para a normalização da atividade cortical em várias disfunções neurológicas.

Após um IS, a HF-rMS reduz a perda neuronal, a morte glial, o volume de enfarte, aumenta a neurogénese, promove a plasticidade sináptica e modula a expressão génica. O nosso grupo demonstrou que a aplicação da HF-rMS a culturas corticais sujeitas a isquemia reduz a morte celular, a degeneração das neurites e modula os marcadores sinápticos, sendo os astrócitos cruciais para os efeitos benéficos observados. Observou-se ainda que a aplicação do meio condicionado por astrócitos é suficiente para a indução dos efeitos benéficos. Apesar de vários estudos terem mostrado a capacidade da rMS em estimular a libertação de vários fatores tróficos para o meio, os componentes libertados pelos astrócitos em resposta à rMS, e que contribuem para o efeito neuroprotetor não são conhecidos. O objetivo do presente trabalho é determinar os efeitos desencadeados pela HF-rMS nos astrócitos que contribuem para a sua ação neuroprotetora e identificar que mediadores são libertados por estas células em resposta à HF-rMS. Utilizando culturas de astrócitos e culturas de neurónios e astrócitos corticais sujeitos a OGD

avaliámos o efeito da HF-rMS nos níveis de transportadores de glutamato EAAT1 e EAAT2, e nos níveis de fatores de crescimento libertados para o meio celular.

A avaliação dos níveis dos transportadores de glutamato EAAT1 e EAAT2 nos astrócitos mostrou que o EAAT2 não foi afetado pela HF-rMS, contudo, o EAAT1 aumentou em culturas sujeitas a OGD e HF-rMS, sugerindo que a neuroprotecção promovida pela HF-rMS pode envolver uma redução da excitotoxicidade. Além disso, a HF-rMS aplicada após OGD aumentou os níveis celulares de mRNA de Gdnf e de proteína GDNF, e a HF-rMS promoveu a libertação de GDNF pelos astrócitos. Para avaliar a contribuição do GDNF libertado pelos astrócitos em resposta à HF-rMS para a neuroprotecção mediada pela estimulação após um episódio de OGD, neutralizámos o GDNF presente no meio condicionado por astrócitos por ação de um anticorpo anti-GDNF. Não se observaram diferenças na viabilidade celular após HF-rMS, analisada através do ensaio de MTT e, por seguinte, também não se observaram efeitos da neutralização do GDNF. Contudo, estes dados vão de encontro ao que foi observado anteriormente pelo nosso grupo, ou seja, a HF-rMS não aumenta a viabilidade celular, mas contribui para a recuperação dos neurónios sobreviventes. Através da análise Sholl verificou-se que a neutralização de GDNF impediu a recuperação do número e do comprimento de neurites promovida pela HF-rMS. Além disso, a neutralização de GDNF impediu ainda o aumento do número de neurónios c-Fos^{+} induzido pela HF-rMS. Resumidamente, estes resultados sugerem que a HF-rMS é capaz de promover a recuperação neuronal através da promoção da libertação de fatores tróficos para o meio, entre eles o GDNF. Os dados obtidos sugerem ainda que a HF-rMS poderá proteger os neurónios da excitotoxicidade glutamatérgica, uma vez que induz um aumento da expressão de EAAT1.

A modulação dos efeitos protetores mediados pelos astrócitos por ação da HF-rMS poderá ser uma estratégia útil em patologias em que há lesão neuronal, e mostram que a ação protetora desta técnica se estende para além dos processos de regulação da atividade elétrica das redes neuronais.

Palavras-chave

Acidente vascular cerebral isquémico; estimulação magnética repetitiva de alta frequência; astrócitos; neuroprotecção; GDNF.

Abstract

Ischemic stroke (IS) is caused by the reduction or blockage of blood flow to the brain and is the third most common cause of death in Portugal. Due to its ability to improve the most frequent clinical sequelae left by brain ischemia, high-frequency repetitive transcranial magnetic stimulation (HF-rTMS) has been considered a promising therapeutic strategy for IS. The observed improvements have been associated with changes in neurons and their synaptic liaisons. However, the hypothesis that this technique modulates astrocytes, potentiating their neuroprotective capabilities, was also raised. With the present work, we aim to clarify which mechanisms triggered by high-frequency repetitive magnetic stimulation (HF-rMS) in astrocytes contribute to its neuroprotective effects.

Neuron-glia and astrocyte cortical cultures subject to oxygen and glucose deprivation were used as an *in vitro* model of ischemia. Neuroprotection promoted by HF-rMS was evaluated through the analysis of markers of neuronal activity and morphometric analysis of neurons. The levels of growth factors in the astrocyte-conditioned medium (CM) were assessed through a Growth Factor Array and glial-derived neurotrophic factor (GDNF) expression was analyzed by RT-PCR and Western Blot.

Our results show that neurons injured by ischemia can be rescued through the modulation of astrocytes by HF-rMS. This modulation helps to maintain the number and length of neurites and increases the number of neurons expressing c-Fos. Quantification of glutamate transporters EAAT1 and EAAT2 in astrocyte extracts showed that EAAT2 levels were not affected by HF-rMS, however, EAAT1 levels were increased in cultures subjected to OGD and HF-rMS, suggesting that HF-rMS neuroprotection may involve a reduction of excitotoxicity. Furthermore, analysis of the astrocyte CM showed that HF-rMS stimulated the release of several trophic factors by astrocytes, namely GDNF. Neutralization of GDNF present in the CM impeded the recovery of neurite number and length induced by HF-rMS and blocked the increase of c-Fos$^+$ neurons, indicating that this neurotrophic factor plays a crucial role in the neuronal recovery induced by HF-rMS.

Our results show that modulation of astrocytes by HF-rMS effectively rescues neurons injured by ischemia by decreasing excitotoxicity and promoting neuroprotection through the release of GDNF by the astrocytes. This suggests that by targeting astrocytes, HF-rMS can be used to promote neuroprotection in other brain lesions.

Keywords

Ischemic stroke; high-frequency repetitive magnetic stimulation; astrocytes; neuroprotection; GDNF.

Publications

Submitted Article:

- **High-frequency repetitive magnetic stimulation rescues ischemia-injured neurons through modulation of glial-derived neurotrophic factor present in the astrocyte's secretome**
  Genilso Gava-Junior [1#], Susana A. Ferreira [1#], Cláudio Roque [1,2], Julieta Mendes-Oliveira [1], Inês Serrenho [1], Nuno Pinto [1,2], Maria Vaz Patto [1,2] and Graça Baltazar [1,2*] submitted to Journal of Neurochemistry
  [#]The authors contributed equally to this work

Article under internal review:

- **The modulatory effects of repetitive transcranial magnetic stimulation on non-neuronal cells: a systematic review**
  Susana A. Ferreira [1], Nuno Pinto [1,2], Inês Serrenho [1], Maria Vaz Patto [1,2], and Graça Baltazar [1,2*]

Index

List of Figures

List of Abbreviations

AMPA	α-amino-3-hydroxy-5-methyl-4-isoxazolepropionic acid
ATP	Adenosine triphosphate
BDNF	Brain-derived neurotrophic factor
CiA	Cyclophilin a
CM	Conditioned medium
cTBS	Continuous theta-burst stimulation
DIV	Days *in vitro*
EAAT1	Excitatory amino acid transporter 1
EAAT2	Excitatory amino acid transporter 2
FBS	Fetal bovine serum
GAPDH	Anti-glyceraldehyde-3-phosphate dehydrogenase
GDNF	Glial cell line-derived neurotrophic factor
GLAST	Glial glutamate and aspartate transporter
GLT-1	Glial glutamate transporter
HBSS	Hank's balanced salt solution
HF-rMS	High frequency repetitive magnetic stimulation
HF-rTMS	High frequency repetitive transcranial magnetic stimulation
HRP	Horseradish peroxidase
iTBS	Intermittent theta-burst stimulation
LF-rTMS	Low frequency repetitive transcranial magnetic stimulation
LTD	Long-term depression
LTP	Long-term potentiation
MCAO	Middle cerebral artery occlusion
MEP	Motor evoked potential
MTT	3-(4,5-dimethylthiazol-2-yl)-2,5-diphenyltetrazolium bromide
NMDA	N-methyl-d-aspartate
OGD	Oxygen and glucose deprivation
PBS	Phosphate buffered saline
PCR	Polymerase chain reaction
PDGF-BB	Platelet-derived growth factor bb
PDL	Poly-D-lysine
rMS	Repetitive magnetic stimulation
rTMS	Repetitive transcranial magnetic stimulation
rtPA	Recombinant tissue plasminogen activator

RT-PCR	Reverse transcription polymerase chain reaction
SDS-PAGE	Sodium dodecyl sulphate polyacrylamide gel electrophoresis
TBS	Theta-burst stimulation
TBS-T	Tris buffered saline with 0.1% tween
TGF-β	Transforming growth factor beta
TMS	Transcranial magnetic stimulation
TNF	Tumor necrosis factor
VEGF	Vascular endothelial growth factor

Chapter 1

Introduction

1. Introduction

1.1. Stroke

1.1.1. Stroke prevalence

Worldwide, 15 million people suffer a stroke annually, with one-third of these people dying and one-third becoming permanently disabled [1]. If not promptly reversed, ischemic stroke (IS) leads to lifelong sequelae that may compromise physical, cognitive, and emotional functions [1, 2]. A quarter of adults over the age of 25 are expected to suffer an IS in their lifetime, with a large percentage retaining sequelae that will severely compromise their quality of life [3]. In the European Union, stroke is the second leading cause of death and one of the main causes of disability in adulthood, and in Portugal, the third leading cause of death, only surpassed by cardiovascular diseases and cancer, with more than 14,000 cases documented annually [4, 5].

1.1.2. Ischemic stroke and hemorrhagic stroke

An IS arises due to a decreased or blockage of the blood flow to brain tissues due to cerebral infarction caused by a thrombus [6]. Embolism is the main cause of IS, with most emboli being clots formed in the heart (cardiac embolism) [7]. A hemorrhagic stroke is defined as an acute neurological injury that occurs due to bleeding in the brain and can be divided into two mechanisms: intracerebral hemorrhage, in which there is bleeding in the brain, or subarachnoid hemorrhage, in which there is bleeding in the space that surrounds the brain [8].

Although hemorrhagic stroke is more deadly, IS is more common [8]. Of all strokes, 87% are ischemic, 10% are hemorrhagic, and 3% are due to subarachnoid hemorrhage [9].

1.1.3. Post-stroke impairments

As mentioned before, if not promptly reversed, ischemic stroke (IS) leads to lifelong sequelae that may compromise physical, cognitive, and emotional functions, depending on the location, size, and severity of the injury [1, 2].

Common complications after stroke include both short-term complications and long-term sequelae. The physical impairments consist of motor, visual and somatosensory deficits. Motor deficits include paralysis or deficit of neuro-musculoskeletal function which can lead to reduced joint mobility or muscle strength, spasticity, hemiplegic shoulder pain, wrist and hand flexion [10, 11], or dysphagia [12].

The visual impairments can cause visual loss, monocular or binocular [13]. The somatosensory deficits consist of numbness or tingling in one part of the body, in less severe cases, to complete sensory neglect of a body part or one side of the body, in the most severe cases [14]. Cognitive impairments can include deficits in memory, concentration, attention, and orientation [15, 16]. Emotional impairments are more subtle, but with considerable impact on life quality. IS patients may experience anxiety, frustration, anger, sadness, and depression [17, 18].

1.1.4. *In vivo* and *in vitro* models of ischemic stroke

There are several models, both *in vivo* and *in vitro* to mimic IS. *In vivo* studies are mainly done in rats and there are several different models, however, the most widely used are the middle cerebral artery occlusion (MCAO) model and the photothrombosis model. The MCAO model consists of introducing a monofilament through the internal carotid artery to block the middle cerebral artery during 1 to 2 hours, followed by reperfusion. The longer the monofilament stays in, the more extensive the injury will be [19, 20]. In the photothrombosis model, the photosensitive dye Rose Bengal is injected intraperitoneally, and then a part of the brain is illuminated with a specific wavelength of light, which will form highly reactive oxygen products that in turn induce peroxidation of the endothelial cell membranes, leading to platelet adhesion and aggregation, and eventually to thrombus formation leading to interruption of local brain flow. The light source can be applied to the intact skull without the need for craniotomy, which allows targeting any cortical area of interest in a reproducible and non-invasive way. Photothrombosis does not obstruct just one artery as usually happens in the case of human stroke and induces lesions in superficial vessels [21, 22].

Another option is a craniotomy model, which consists of directly ligating, clamping, or cauterizing the brain vessel, however, this model is quite different from what occurs in humans and causes more trauma to the animals [23, 24]. The endothelin-1 model is another model used. Endothelin-1 is a peptide with vasoconstrictor properties, which when applied directly to the blood vessel, will lead to its vasoconstriction causing ischemia, furthermore, when the effect wears off, the blood flow is restored representing reperfusion. However, this model also does not mimic a human stroke due to the reduced edema [22, 23]. Finally, there are also models of embolic stroke, which can be of two categories: thromboembolic clot models or models induced by micro or macro spheres. Thromboembolic clots consist of the injection of pre-formed clots or the injection of thrombin directly into the internal carotid artery or middle cerebral artery, which will induce clot formation. The micro- or macro-sphere models, on the other hand, consist of

injecting micro-spheres (20-50µm) or macro-spheres (300-400µm) that will in turn block the blood circulation [23, 24].

As for *in vitro* models, there are two: oxygen and glucose deprivation (OGD) and chemical or enzymatic inhibition of metabolism. The chemical or enzymatic inhibition methods use rotenone, antimycin, or sodium azide to inhibit the electron transport chain. The cell damage mediated by antimycin was the most reproducible, however, and despite this being an easy and fast method, it causes the release of many free radicals, so it is not very suitable for ischemic stroke studies. The most widely used method is oxygen and glucose deprivation, which consists of changing the cell culture medium to a glucose-free medium and place the cell culture in a closed chamber in an N_2/CO_2 atmosphere for 1 to 24 hours. The longer the OGD takes, the bigger the cellular damage will be. Then, the medium is replaced, and the cells are placed back in a CO_2 incubator, mimicking the reperfusion phase. This model reproduces more closely what happens in IS [23, 25].

1.1.5. Ischemic stroke cascade of events

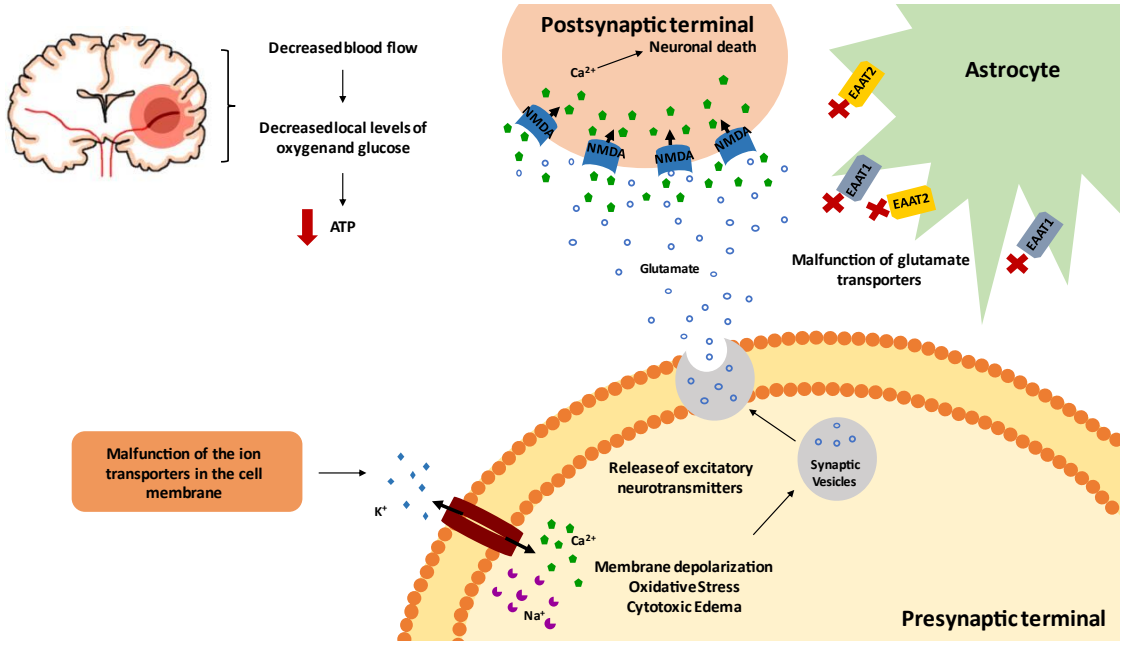

Figure 1 Cascade of cellular events after IS that lead to cell death. Ischemic injury results from a set of cellular and molecular events caused by a decrease or loss of blood flow in a particular region of the brain. This set of events is called the ischemic cascade and consists of a cellular energy failure, followed by excitotoxicity, oxidative stress, blood-brain barrier dysfunction, and post-ischemic inflammation (these last two are not represented in the figure), which together contribute to cell death. In the first few minutes, the shortage of blood flow produces an energy gap in brain cells, which causes membrane depolarization, triggering the release of the neurotransmitter glutamate into the synaptic cleft. The overactivated postsynaptic N-methyl-D-aspartate (NMDA) receptors will lead to excitotoxicity processes (mainly due to Ca^{2+} influx). In addition, energy failure and depolarization of the cell membrane inhibit glutamate transporters in astrocytes and may even induce a reverse function of their action leading to further release of glutamate into the synaptic cleft.

IS is characterized by a lack of oxygen and glucose in a part of the brain. This failure of oxygen and glucose in the cells will start a cascade of events that will lead to cell death [6, 26].

Initially, the lack of oxygen in the brain will lead to reduced ATP due to decreased or stopped oxidative phosphorylation. Insufficient glucose will lead to the utilization of brain glycogen, which is mostly provided by astrocytes, however, this quickly runs out. In addition, oxygen insufficiency leads to anaerobic glycolysis, which produces a large amount of lactate. The lactate can be used as an energy substrate for neurons, but also leads to intracellular acidification [6, 26].

The cessation of oxidative phosphorylation triggers the reversion of ATP synthase accelerating ATP consumption and triggering the production of reactive oxygen species [6, 26].

As shown in Figure 1, the ATP depletion will compromise functioning of membrane ion transporters, as is the case of the NA^+/K^+ pumps, which leads to a decrease in intracellular K^+ and an increase in the levels of Cl^-, Ca^{2+} and Na^+ inside the cells. The increase of intracellular Na^+ will lead to an increase of H_2O inside the cell, causing cytotoxic edema that can lead to membrane rupture, while the increase of Ca^{2+} will cause mitochondrial disfunction that will induce the release of apoptotic factors and degradative enzymes [6, 26].

Consequently, cellular depolarization occurs, leading to activation of voltage-dependent calcium channels, and release of excitatory neurotransmitters into the extracellular space, such as glutamate. Due to the dysfunction of the NA^+/K^+ pump, the transport of glutamate is hampered, causing its accumulation in the synaptic cleft. This leads to the continuous stimulation of postsynaptic receptors, such as the N-methyl-D-aspartate (NMDA) receptors, which leads to the loss of calcium homeostasis and the activation of intracellular events that culminate in cell death, a process known as glutamatergic excitotoxicity [6, 26]. Furthermore, the energy failure and cell membrane depolarization, inhibits glutamate transporters in astrocytes and could even induce its reverse function leading to further glutamate accumulation in the extracellular space [27].

After several hours, the immune cells start to remove the damaged cells, a process that triggers inflammation. This inflammation alters the blood-brain barrier allowing fluids and proteins to enter the brain and causing edema. The increased inflammation also leads to the release of cytokines and chemokines that exert deleterious effects on the neurovascular network [6, 26].

All these processes, energy failure, excitotoxicity, oxidative damage, and inflammation contribute to cell death [6, 26].

1.1.6. Phases of ischemic stroke: acute, subacute, and chronic

There are three phases after a stroke, the acute phase, the sub-acute phase, and the late phase. The decrease in cerebral blood flow and the reduction of oxygen and glucose initiates the processes of the acute phase, where intracellular levels of Ca^{2+}, Na^{+}, and Cl^{-} increase, oxidative stress, and glutamatergic excitotoxicity also increase and the expression of glutamate transporters is promoted. The subacute phase is characterized by the occurrence of various forms of cell death, the blood-brain barrier becomes more permissive, and an inflammatory response is triggered. In the late phase, the glial scar develops, allowing a demarcation between the infarct zone and the penumbra zone, and recovery processes begin in the surrounding area with the occurrence of angiogenesis, neurogenesis, and re-myelination [6, 26].

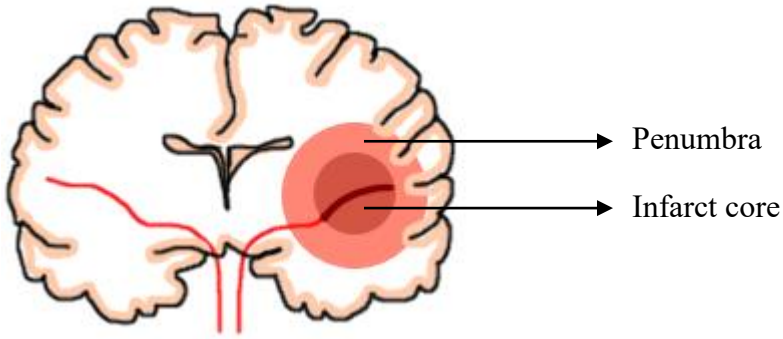

Figure 2 Representation of the core and penumbra region after an IS. The core of the infarct is the region in which the severe decrease in blood flow causes an energetic failure, and therefore the cells quickly die of necrosis. In contrast, the penumbra is the region where although death pathways by apoptosis is activated, if reperfusion occurs, the tissue has the possibility of being preserved. If this reperfusion does not occur, the infarct core expands into the penumbra.

The infarct core and the penumbra zone are formed still in the acute phase and are represented in Figure 2. The infarct core is the area where the reduction of blood flow has occurred and presents almost immediate irreversible damage with total cell death by necrosis due to the reduction of oxygen and glucose. The penumbra zone is an area of tissue that has been exposed to a moderate decrease in blood flow, which makes the penumbra a zone of progressive damage to neuronal tissue, in the course of hours or days. The penumbra zone is the focus of stroke treatments due to its recovery potential. However, the progression of ischemic damage is time-dependent, so the sooner a patient treated, the better the prognosis [6].

1.1.7. Effects of ischemia on brain cells: neurons and glia

The brain is extremely susceptible to ischemia because neurons are cells with high energy requirements and therefore, the interruption of blood flow for only a few minutes leads to a cascade of events that triggers neuronal death [28]. Microglia comprise 10-15% of all cells in the brain and constitute the first defense line in the central nervous system [29]. Activated M1 microglia is the first step in the inflammatory response after IS and this activation is initially triggered by neuronal death. In the acute phase, activated microglia secrete several inflammatory cytokines (tumor necrosis factor (TNF), IL-1β, and IL-6) that contribute to the inflammatory response. After the acute phase, microglia take over the repair function by removing the injured neurons [30, 31]. M2 microglia release anti-inflammatory cytokines that restore tissue homeostasis [29]. Astrocytes account for 50% of the brain cells [29]. M1 microglia induces A1 astrocyte phenotype that trigger neuronal damage [30]. The cytokines released by cells in the zone of injury and penumbra, lead to the formation of the glial scar by reactive astrocytes, a scar that restricts the spread of neuroinflammation and inhibits axonal regeneration [29, 30].

There are also A2 astrocytes that release neurotrophic factors with neuroprotective effects by releasing anti-inflammatory cytokines and trophic factors, such as brain-derived neurotrophic factor (BDNF), glial cell line-derived neurotrophic factor (GDNF) or vascular endothelial growth factor (VEGF) [29, 30]. Oligodendrocytes constitute 5-8% of total adult brain glial cells. Oligodendrocytes are extremely sensitive to excitotoxicity and oxidative stress produced during ischemia, which can lead to demyelination. This demyelination causes axonal destabilization and alters neuronal communication. These events are aggravated by M1 microglia and A1 astrocytes. On the contrary, trophic factors released by M2 microglia and A2 astrocytes increase oligodendrogenesis [29].

1.1.8. Glutamate and excitotoxicity in ischemia

Glutamate is the main excitatory neurotransmitter in the brain. Glutamate is released by vesicles present at the presynaptic terminals in a Ca^{2+}-dependent manner. Postsynaptically, it acts on three families of ionotropic receptors, the NMDA, the α-amino-3-hydroxy-5-methyl-4-isoxazolepropionic acid (AMPA), and the kainate receptors, although the permeability to Na^{+} and Ca^{2+} is different between each receptor, all of them promote the influx of cations. In addition to ionotropic receptors, glutamate also acts on metabotropic receptors which consist of three classes, with class I receptors regulating phospholipase C and leading to the production of diacylglycerol and inositol

triphosphate, and class II and III receptors being negatively coupled to adenylyl cyclase [32, 33].

In a normal condition, glutamate is released into the synaptic cleft and captured by membrane glutamate transporters. Astrocytes are the main cells responsible for the uptake and recycling of glutamate. Glutamate is collected and converted into glutamine, which can then be used by neurons for glutamate synthesis. This function is essential to ensure correct function of glutamatergic synapses [29].

There are five types of glutamate transporters, two of which are expressed predominantly in astrocytes, excitatory amino acid transporter 1 (EAAT1) and excitatory amino acid transporter 2 (EAAT2), also known as glial glutamate and aspartate transporter (GLAST) and glial glutamate transporter (GLT-1), and three are expressed in neurons: excitatory amino acid carrier 1 (also known as EAAT3 in humans), EAAT4 and EAAT5 [32, 33]. Although glutamate transport normally occurs in the direction of glutamate entry into the cell, however in cases of IS in which Na^+ and K^+ gradient across the membrane is reduced, especially in the core area, the reverse function of glutamate transporters can be induced, further increasing excitotoxicity [29].

1.1.9. Growth factors in ischemia

Growth factors are biologically active molecules, mainly peptides or proteins, that affect the regulation of several organic processes, namely, the inflammatory process, coagulation, healing, and cell differentiation and proliferation. Growth factors are also essential for cell survival, neurogenesis, differentiation, synaptogenesis, and neuroprotection [34-37].

After ischemia, the increased expression of growth factors, specially BDNF, GDNF, platelet-derived growth factor (PDGF), and VEGF, activates a cascade of signaling pathways that regulate angiogenesis, inflammation, cell differentiation, proliferation, and apoptosis and promote neuronal plasticity and functional recovery [34-37].

1.1.10. Stroke treatments in acute and chronic phase

Since stroke is caused by a decrease in blood flow in one region of the brain, mostly caused by a clot, the current treatment for acute IS aims to restore blood flow as quickly as possible. This reperfusion can be accomplished by administering anticoagulants, such as recombinant tissue plasminogen activator (rtPA), or by extracting the clot surgically. However, not all patients are eligible to take this treatment

since rtPA has a therapeutic window of three to four and a half hours due to the risk of causing a hemorrhagic stroke [38, 39].

In the chronic phase of stroke, besides the use of medication to treat possible medical complications, the therapies that are most recommended to reduce the disabilities caused by an IS are, depending on the patient's disability, physiotherapy and/or speech therapy [16].

Nevertheless, several innovative therapies are being studied, such as the use of nanoparticles and hydrogels to delivery encapsulated therapeutic biological factors, anti-inflammatory drugs [40], stem cell therapy [41], or gene therapies that offers the potential to alter cellular and molecular processes. Gene therapies are important to recovery from ischemic stroke, reducing the inflammatory response and initiating regeneration of damaged tissue [42]. Among the new therapies, repetitive transcranial magnetic stimulation (rTMS) stands out as a promising non-invasive neuro-modeling strategy for recovery of stroke patients, with several clinical studies showing that this therapy had beneficial results in patients in the chronic phase [43]. rTMS was shown to have beneficial effects on the rehabilitation of limb motor function in both acute and chronic stages of the disease, dysphagia in the post-acute stage, aphasia, hemispatial neglect, depression, and cognitive deficits [43-45].

1.2. Repetitive Transcranial Magnetic Stimulation

1.2.1. Principles of repetitive Transcranial Magnetic Stimulation

Transcranial magnetic stimulation (TMS) is based on the principles of electromagnetic induction, discovered by Michael Faraday in 1831 [46]. TMS is a neurophysiological procedure that consists of applying a magnetic field of time-varying intensity to the superficial layers of the cerebral cortex, causing small internal electrical currents called Eddy currents. Eddy currents allow the stimulation of neurons giving rise to action potentials that either facilitate or inhibit the brain region that is stimulated [47]. Because the impedance of gray matter is higher than in white matter, the electrical current is weaker in the subcortical layers, and therefore, structures such as the thalamus and basal ganglia are not activated by TMS. The effect of TMS is due to the force that the induced electric field exerts on the ionic charges in the intra- and extracellular media of neurons [48]. Although its mechanisms of action are still not entirely clear, TMS has been used for various purposes, such as for brain functional imaging and mapping studies of the cortical cortex, prognosis, or therapeutic uses. One of its great advantages as a therapy is that it has a localized effect and does not influence other organs, unlike oral medication [46, 49].

However, TMS has associated risks, as it can cause convulsions, headaches, transient acute hypomania, or fainting. It also has contraindications, as it is not recommended for patients with pacemakers, metal objects in the skull, or a history of epilepsy [50].

1.2.2. Several types of TMS protocols and different types of coils

The electric field generated by TMS depends on several factors such as the shape and orientation of the coil, the number of turns of the coil, the wave of the magnetic pulse, the intensity, the frequency, the stimulation pattern, and the variation of the magnetic field [48, 51].

The geometry and position of the coil determines the distribution and the focality of the induced electric current in the brain. Circular coils and figure-of-eight coils are the most commonly used, the latter being able to reach a more focal zone in the brain allowing mapping of cortical function, as they allow for high precision stimulation in a small area of the cortex. The focus of the figure-eight coils is located under the intersection of the two constituent circles, as observed in Figure 3.a [48, 51].

TMS is broadly related to neuronal plasticity, the ability of the brain to change its response to stimuli, and more specifically to synaptic plasticity, the ability of each neuron to adapt after each stimulus. Synaptic plasticity includes long-term potentiation (LTP) and long-term depression (LTD) [52, 53]. Depending on the stimulation parameters, TMS can excite or inhibit neurons. TMS can be performed as a form of single pulses or pulse trains, with the latter form seeming to produce more profound changes in neuronal activity [51]. Among the various applications of TMS, rTMS stands out for therapeutic uses. There are two conventional types of rTMS described as low-frequency rTMS (LF-rTMS) and HF-rTMS. While LF-rTMS uses stimulation frequencies lower than 1 Hertz (Hz) and is characterized by continuous trains of single pulses, the HF-rTMS uses stimulation frequencies higher than 5Hz and is characterized by trains of stimuli lasting 5-10 seconds (s) separated by pauses of 20 to 50s [48, 50]. The functional effects of rTMS last longer than just the treatment protocol period, being these effect associated with LTD induced by LF-rTMS and to the LTP induced by HF-rTMS [48]. In addition to these conventional forms of rTMS, there is also an alternative approach, which is delivered in the form of a theta pulse, the Theta-Burst stimulation (TBS). This type of rTMS consists of short bursts of 3 low-intensity pulses of 30 to 100Hz that occur every 200 milliseconds [50, 54]. There are two forms of TBS, the intermittent (iTBS) and the continuous (cTBS). While iTBS delivers a stimulus during 2s every 10s, for 200s total, and can result in MEP

facilitation, the cTBS delivers a continuous stimulus for 40s, which can result in MEP inhibition [55]. All these stimulation protocols are represented in Figure 3.b.

However, although TMS is mainly associated with LTP and LTD processes, other mechanisms of action have been described. The LTP and LTD processes are related to the electric current induced by TMS, causing changes in synaptic plasticity and neurotransmitter release, as previously mentioned. However, several studies have shown that the intrinsic magnetic field is also responsible for several effects including macromolecular magnetic effects, magnetic spin effects, genetic magnetoreception, and quantum effects, which affect the genetic apparatus of cells, modulate neuroprotection, affect the release of neurotrophic factors, and modulate glial cells. Furthermore, the combination of the induced electric current and the intrinsic magnetic field is seen as the possible explanation for the long-term effects caused by rTMS [56].

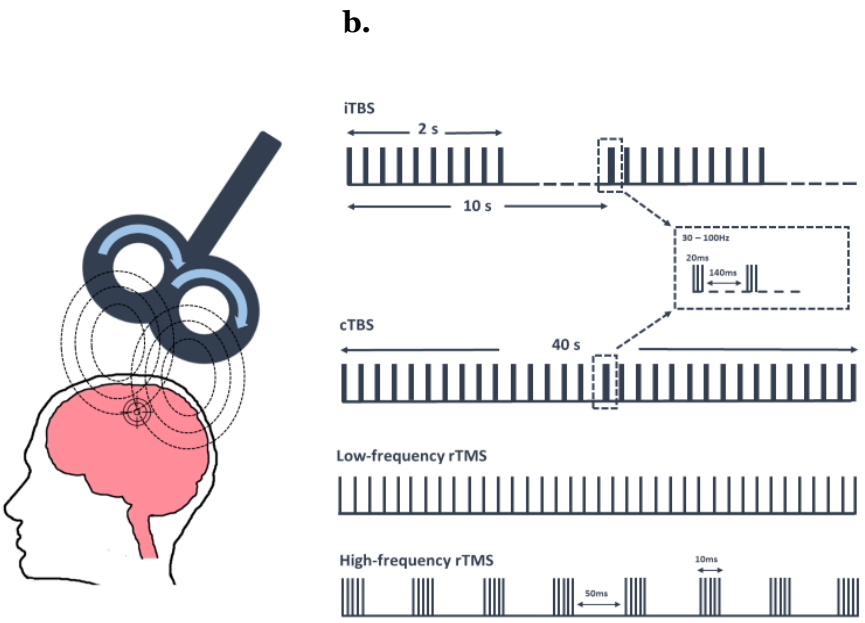

Figure 3 Representation of the TMS application and protocols. (**a**) For the application of TMS, an electric current is passed through the turns of wire that make up the coil. The coil is placed above the scalp and the magnetic field lines produced by the electric current are formed perpendicular to the coil. An induced electric field is formed perpendicular to the magnetic field, and therefore parallel to the coil. The focus of the largest induced current is located under the intersection of the two round components of the coil. (**b**) Representation of the pulses given in each stimulation protocol. Theta Burst Stimulation consists of trains of 30 to 100Hz pulses that occur every 200ms. In the iTBS protocol, the bursts last 2s and are repeated every 10s, while in cTBS the bursts are repeated every 40s and there are no pauses. At low frequency (<1Hz) there is a decrease in cortical excitability, while at high frequency (>5Hz) there is an increase in cortical excitability.

1.2.3. Effects of HF-rMS in glial cells

HF-rTMS induces a transient increase in GFAP expression, increasing few days after stimulation, and returning to basal levels after a few days or weeks, which indicates that HF-rMS does not modulate astrocyte reactivity in lesion-free models [57-60].

Regarding astrocyte activity, intracellular calcium levels were analyzed. Intracellular calcium is a major regulator of astrocytes and the capacity of HF-rMS to alter calcium levels of astrocytes was also studied [61, 62]. Although Clarke and colleagues (2017) did not observe differences in intracellular calcium levels [61], the same group reported that HF-rMS decreased the expression of stromal interaction molecule 1, calcium release-activated calcium modulator 3, and calcium-activated potassium channel subunit beta-4, proteins involved in the regulation of intracellular calcium [62].

Concerning oligodendrocytes, exposure of induced pluripotent stem cells cultures to HF-rMS resulted in an increase of oligodendrocyte proliferation, as well as oligodendrocyte differentiation from progenitor cells, demonstrated respectively by increased oligodendrocyte transcription factor 2 transcription [63], and activation of the non-canonical transforming growth factor β (TGF-β)-Akt and TGF-β-Erk1/2 pathways, known to mediate oligodendrocyte differentiation and myelination [60].

1.2.4. Use of HF-rMS in Neurological Disorders

Over recent years, rTMS has been proposed to be used as a therapeutic approach for several neurological disorders such as major depressive disorder, IS, Parkinson's disease, Alzheimer's disease, and multiple sclerosis [64]. In patients with major depressive disorders, rTMS was associated with a decrease in the severity scores and to an improvement of depressive symptoms [43]. Clinical data shows that rTMS is capable of reducing functional deficits frequently presented by in IS patients, namely reduced limb motor function [65], aphasia [66], hemispatial neglect [67], dysphasia [68], and cognitive deficits [69]. In Parkinson's Disease, clinical studies show a reduction of tremor, rigidity, bradykinesia, dyskinesia, postural instability, and gait performance [70-74]. In Alzheimer's Disease patients, rTMS was associated with improvement of memory and learning [75, 76], and in multiple sclerosis, rTMS reduced fatigue [77], pain and inflammation [43].

The Food and Drug Administration has already indicated TMS as an accepted treatment for drug resistant major depressive disorder and obsessive-compulsive disorder [53].

Concerning the impact of HF-rMS on glial cells in disease models, astrocyte reactivity decreased in Alzheimer's Disease [78], chronic pain [79, 80], hemorrhagic stroke [81], IS [82], multiple sclerosis [83], spinal cord injury [84-86] and traumatic brain injury [87]. Microglia reactivity was also affected and showed reduction in Alzheimer's Disease [78, 88], IS [89], multiple sclerosis [90], and spinal cord injury [84,

86, 91]. The inflammation decreased in Alzheimer's Disease [88], IS [82, 89], and multiple sclerosis models [90, 92]. Oligodendrocytes are also affected by HF-rMS with increases of proliferation, differentiation, and myelination observed in multiple sclerosis [90, 92] and in spinal cord injury models [84, 91].

1.2.5. Use of HF-rMS in post-stroke patients

TMS is being increasingly used for post-stroke motor rehabilitation due to its ability to model excitability in the cortical motor network and to interfere with neuronal plasticity [53, 93]. One strategy used is to apply HF-rTMS to the ipsilateral motor cortex to enhance reperfusion and brain reorganization leading to synaptic plasticity, particularly of the synapses necessary for movement control. However, another strategy is to apply LF-rTMS to the contralateral motor cortex in order to decrease the inhibition exerted on the ipsilesional side. Either of these strategies seems to have positive consequences on motor learning [53, 93].

TMS is often combined with physical therapy as TMS appears to increase the recovery process. Several clinical studies have examined the potential of TMS to treat motor dysfunction and aphasia in post-stroke patients [44]. Chieffo and colleagues (2014) studied the ability of HF-rTMS to improve chronic aphasia in post-stroke patients and a significant improvement was noted [94]. Another study from the same group evaluated 10 patients who suffered cortical strokes and had lost the full walking ability, and improvements in lower limb motor function were observed [95]. Wang and colleagues (2020) evaluated 15 stroke patients treated with HF-rTMS and noted improved recovery of motor impairment with stimulation in the contralesional hemisphere [96]. Sasaki and colleagues (2013) compared five days of LF-rTMS in the contralesional hemisphere with the application of HF-rTMS in the ipsilesional hemisphere and found that HF-rTMS increased motor function recovery [97].

1.2.6. How does HF-rMS affects glial cells and neurons in cerebral ischemia?

In addition to the effects that magnetic stimulation has on neurons, there has been increasing mention of the effects that TMS has on glial cells. The modulation of several markers of astrocytic reactivity by HF-rMS was evaluated in different IS models. HF-rMS treatment of primary cortical cultures exposed to OGD and of Sprague-Dawley rats that suffered MCAO induced a decrease in C3 and iNOS and increased S100A10 and Arg1, suggesting a conversion astrocyte with the A1 phenotype into the A2 form [82]. In what concerns the GFAP levels, Luo et al (2017) and Caglayan et al (2019) reported the

absence of alterations, whereas Hong et al (2020) reported a decrease in GFAP levels induced by HF-rTMS [82, 89, 98].

In a study realized by our group, we showed that HF-rMS also prevents neuronal death and neurite degeneration induced by OGD and increases the number of cells expressing ERK1/2 and c-Fos, and the number and intensity of synaptic puncta. Interestingly, these effects were only observed in neuron-astrocytes cultures, and not in neuron-enriched cultures, thus suggesting that astrocytes are essential for the beneficial effects induced by HF-rMS after ischemia [99]. Hong and colleagues (2020) also reported that astrocytes contribute to the beneficial effects of HF-rMS after ischemia and demonstrated that the culture medium from astrocytes that underwent HF-rMS was sufficient to decrease neuronal apoptosis. This study also reported that HF-rTMS decrease the levels of the pro-inflammatory mediator TNF-α and increase the anti-inflammatory mediator IL-10 in the medium, which may contribute to the observed beneficial effects [82]. The same authors observed that the HF-rTMS applied to Sprague-Dawley rats that suffered MCAO reduce infarct volumes, and improved cognitive functions, assessed by modified neurological severity score [82, 89, 98]. Using the MCAO model, Caglayan and collaborators (2019) showed that HF-rTMS reduced neuroinflammation, as showed by decreased expression of inflammation-related genes such as IL-1β, TNF-α, TGF-β and MMP9, and also by a decrease in the number of Iba-1 positive cells [89].

Besides the effects already mentioned, HF-rTMS caused an upregulation of VEGF-A and VEGF-B, which promotes angiogenesis, that in turn protected capillary integrity, observed by an increase in CD31 positive cells [89, 98]. These data suggest that glial cells are crucial targets for the neuroprotection caused by HF-rTMS.

Chapter 2

Objectives

2. Objectives

Although HF-rTMS is applied in patients and has shown beneficial effects, the biological mechanisms behind these effects are not yet fully understood. Most of the existing data on the application of this technique are focused on the action of this technique in neurons, and data on glial cells are scarce.

A previous work by our group showed that through factors that they released into the medium astrocytes play an important role in neuronal recovery. Thus, the goal of this work is to understand how astrocytes can contribute to the beneficial effects after HF-rMS. More specifically, the present work aims to answer the following points:

1. Is HF-rMS capable to increase glutamate transporters levels, and consequently decrease excitotoxicity?

2. What are the trophic factors that astrocytes release into the extracellular medium after HF-rMS that lead to neuroprotection?

Chapter 3

Materials and Methods

3. Materials and Methods

3.1. Animals

All procedures were approved by the Animal-Welfare body of the Health Research Centre at the University of Beira Interior and followed the requirements of the European Convention for the protection of vertebrate animals used for experimental and other scientific purposes (Directive 2010/63/EU). The rat colony was obtained from Wistar Han IGS rats purchased from Charles River (RRID: RGD_2308816). The animals were bred at CICS-UBI Health Science Research Center animal facilities, with free access to water and food and maintained under a 12-hour light/dark cycle under standard humidity and temperature conditions. Females (220-260 g) were housed in groups of four in individually ventilated cages.

To obtain embryonic brain tissue, pregnant females were anesthetized with ketamine (87.5 mg/kg, Imalgene 1000) and xylazine (12 mg/kg, Rompun), the abdominal cavity was opened, the embryos were removed and then the females were euthanized by exsanguination through a cut in the aorta. Embryos from Wistar rats at the 15^{th}-16^{th} day of embryonic development, used to prepare cortical cultures were taken from the animal facility to the culture room while still in the yolk sac in a 50mL tube with phosphate buffered saline (PBS)[1].

3.2. Culture of astrocytes

Cell culture was performed as previously described [100]. From the moment that the embryos arrived at the culture room, all procedures were carried out inside the laminar flow hood previously disinfected with ethanol 70% and using sterile material.

The embryos were carefully removed from the yolk sac and placed in a Petri dish with cold PBS. Next, the cortices were dissected in another Petri dish with the help of a magnifying glass. The scalp and meninges were removed, the cortex was collected, chopped into small pieces, and pooled together in a falcon with 5 ml of PBS.

Mechanical digestion of the tissue was performed with a micropipette with a regular tip, followed by plastic tips punctured with needles of decreasing diameter (20G: 0.9 mm, 23G: 0.6 mm, and 25G: 0.5 mm). After mechanical digestion, the cell suspension was centrifuged (400 g, 3 minutes), the supernatant was discarded, and the

[1] **Phosphate-buffered saline (PBS):** 140 mM NaCl (Fisher Scientific, S271-500), 2.7 mM KCl (PanReac AppliChem, A2939), 1.5 mM KH_2PO_4 (Honeywell, 60216), and 8.1 mM Na_2HPO_4 (Fisher Bioreagents, BP332-500), pH = 7.2.

pellet was resuspended in 10 ml of M10cG medium[2] for astrocyte-enriched cultures, or in 10 ml of Neurobasal medium[3] for neuron-glial cultures, pre-heated at 37°C. Finally, the cells were cultured in 9.4cm² plates (Thermo Scientific, 130180) coated with poly-D-Lysine (PDL)[4] at a density of 0.1489×10^6 cells/cm² for Western Blot, Growth Factor Array, and 3-(4,5-dimethylthiazol-2-yl)-2,5-diphenyltetrazolium bromide (MTT) analysis and in 24-well plates at a density of 0.11912×10^6 cells/cm² for immunocytochemistry. For the astrocyte-enriched cultures, 3 hours after plating the cultures were washed with cold MEM to kill the neurons.

Each experiment consisted of four experimental groups, the control, which was not subjected to OGD or HF-rMS, the OGD, subjected only to OGD, the HF-rMS, subjected only to HF-rMS, and the OGD + HF-rMS, which was subjected to OGD and HF-rMS.

The cells were kept in culture for 9 days in an incubator with controlled temperature and CO_2 (37°C, 5% CO_2). On the 8th day in vitro (DIV) the cells were exposed to oxygen and glucose deprivation and HF-rMS, and 24 hours after the HF-rMS, both the cell extracts and the conditioned medium (CM) or the coverslips were collected to perform Western Blot, RT-PCR, and MTT assay or to perform the growth factor array and the GDNF neutralization, or immunocytochemistry, respectively (Figure 4).

[2] **M10cG medium:** 9.6 g/L MEM (Sigma-Aldrich, M0268), 0.026 M $NaHCO_3$ (Sigma-Aldrich, S5761), 0.49 mM glutamine (Sigma-Aldrich, G3126), 5 mg/L insulin from bovine pancreas (Sigma-Aldrich, I5500), 3.375 g/L 45% anhydrous D-glucose (Fisher Scientific, G/0450/60), 12 U/ml Penicilin/Streptomycin (Biochrom, A2213), and 10% heat-not inactivated FBS (Biochrom AG, BCS0615), pH=7.2.

[3] **Neurobasal medium:** Neurobasal medium (Gibco, 21103-049), 2% B27 (Gibco, 17504044), 25 µM glutamate (Sigma-Aldrich, G8415), 0.5 mM glutamine (Sigma-Aldrich, G3126), 120 µg/mL gentamicine (Sigma-Aldrich, G1272), and 10% FBS (Biochrom AG, BCS0615), pH=7,2.

[4] **Poly-D-Lysine (PDL):** 0.15 M H_3BO_3 (Chem-Lab, CL00.0216.1000) and 0.1 mg/mL PDL (Sigma-Aldrich, P1149), pH=8.4.

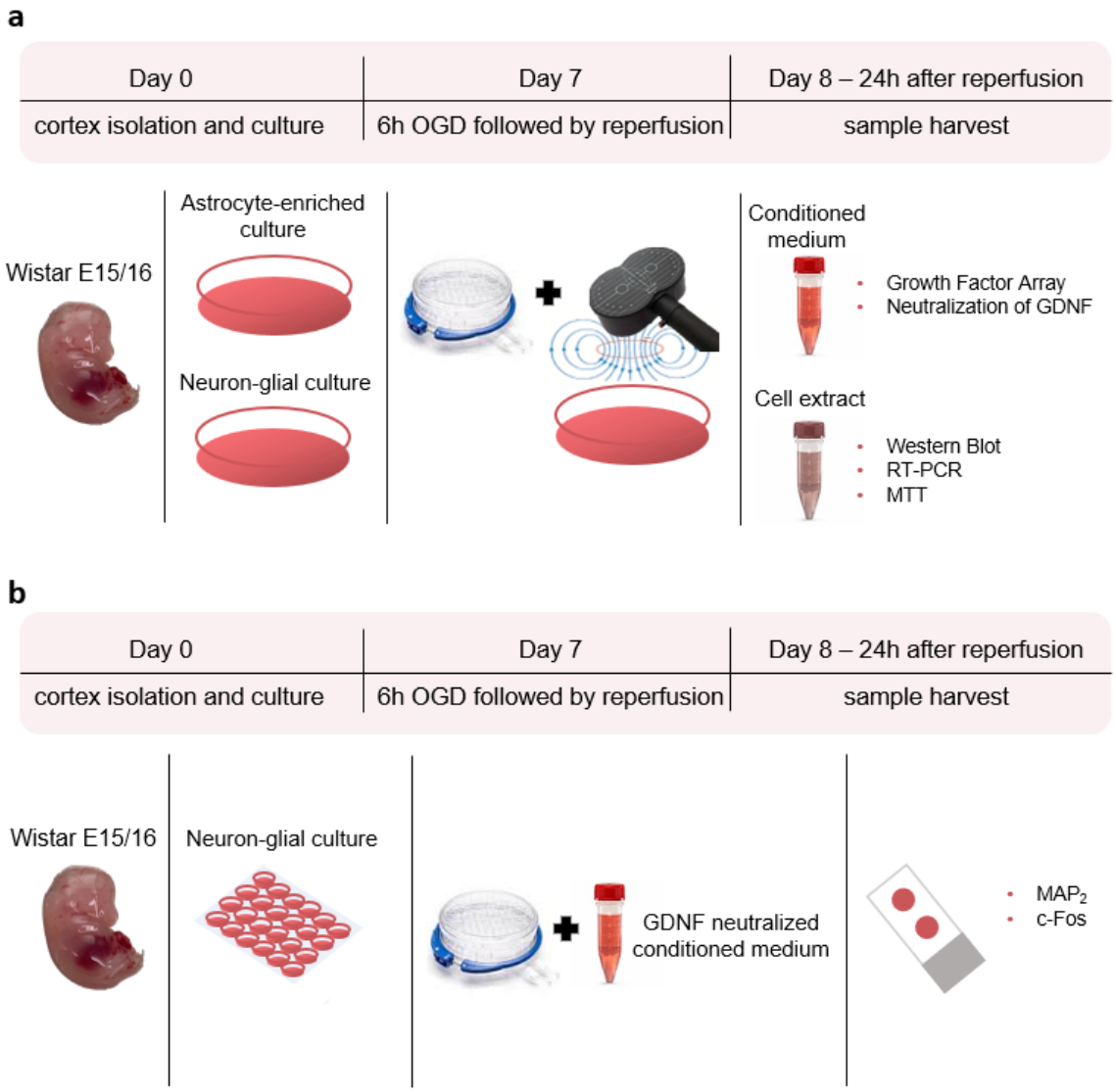

Figure 4 Experimental paradigm. At 8th DIV, the primary cortical cultures were submitted to OGD and HF-rMS, and on 9th DIV both cell extracts and medium were collected for analysis of Western Blot, RT-PCR, MTT assay, immunocytochemistry, growth factor array, and GDNF neutralization.

3.3. Oxygen and Glucose Deprivation and reperfusion

Oxygen and glucose deprivation was performed to simulate what occurs during an ischemic stroke. The protocol was based on procedures previously described [100]. Thus, on the 8th DIV, the culture medium of the cells from the experimental groups exposed to OGD (OGD and OGD + HF-rMS) was removed and replaced by Hank's Balanced Salt Solution (HBSS)[5] without glucose and the culture plates were placed on a hypoxia incubation chamber (Stemcell Technologies, 27310). To induce hypoxia, a 4-minute purge was performed, in which oxygen was replaced by a gas mixture containing

[5] **Hank's Balanced Salt Solution (HBSS):** 1.26 mM $CaCl_2$ (Panreac, C001), 5.36 mM KCl (PanReac AppliChem, A2939), 0.44 mM KH_2PO_4 (Chem-lab, 15004CL0014612), 0.49 mM $MgCl_2$ (LabChem, MGCH-06P-1K0), 139.9 mM NaCl (Fisher Scientific, S271-500), 4.17 mM $NaHCO_3$ (Sigma-Aldrich, S5761), 3.38 mM Na_2HPO_4 (Fisher Bioreagents, BP332-500), and 5.56 mM 45% anhydrous D-glucose (Fisher Scientific, G/0450/60), pH=7.2.

95% N_2 and 5% CO_2 at a flow rate of 20 L/min. After this period, the chamber was sealed, was transferred to an incubator at 37°C, and the cells were left for 6 hours under hypoxia. For the experimental groups not exposed to OGD (control and HF-rMS) the M10cG medium or Neurobasal medium was also removed and replaced by HBSS supplemented with glucose and were placed again in the incubator, under normoxic conditions. After 6 hours the HBSS was removed and replaced by M10cG medium (astrocyte-enriched cultures) or Neurobasal medium (neuron-glial cultures), and the cells were placed back in the incubator. Samples that were used for Western Blot and Growth Factor Array were placed in M10cG medium without fetal bovine serum (FBS), while samples that were used for immunocytochemistry were placed in M10cG medium with FBS.

3.4. High frequency repetitive magnetic stimulation (HF-rMS)

HF-rMS was performed on the 8th DIV right after the medium change that followed OGD. The HF-rMS protocol used throughout this study was based on previous studies of our group [100]. The coil used for stimulation was a figure-8 MCF-B70 coil (180 × 116 mm, 9016E040), connected to a stimulator (MagVenture MagPro X100, 9016E0711). The culture plates were placed under the coil, about 1.5 cm away from the center of the coil, aligning the center of the plate with the center of the coil, thus maximizing magnetic field exposure, and were stimulated. The stimulation protocol consisted of 24 trains of 50 pulses, applied in a biphasic waveform (280 μs duration), delivered at 10 Hz, with a 25s inter-train interval, totalizing 1200 stimuli. Each plate took about 11.5 minutes. The intensity used was about 60% of the maximum device output. Coil temperature ranged between 21 and 37°C, limiting the possible effects of temperature changes. The plates that were not stimulated went to the same stimulation room but were placed away from the stimulating coil.

3.5. Western Blot

Astrocyte-enriched cortical cultures were lysed with cold lysis buffer[6]. Protein concentration was performed with the Bio-Rad Protein Assay (Bio-Rad, 500-0006). After determination of protein concentration samples were denatured by adding loading

[6] **Lysis buffer:** 25 mM Tris (Fisher Scientific, M-27435), 2.5 mM EDTA (Panreac, 131669.1211), 2.5 mM EGTA (Sigma-Aldrich, E4378), 0,2% Triton X100 (Fisher Scientific, BP151-500), 2 mM Na_3VO_4 (Sigma-Aldrich, S6508-10G), 4% complete EDTA free protease inhibitor cocktail tablets (Roche, 04693132001), pH=7.5.

buffer[7] followed by heating at 100°C for 5 minutes. Equal amounts of protein (20µg) were placed in the wells of the gel formed by the stacking gel[8]. Proteins were resolved[9] in a 12% gel by sodium dodecyl sulfate polyacrylamide gel electrophoresis (SDS-PAGE) for 2 hours at 120V in running buffer[10]. After the electrophoresis proteins were transferred[11] at 0.75A, for 80 minutes, to a polyvinylidene difluoride membrane (Amersham™ Hybond® P 0.45). After transference, membrane blocking was performed with 5% non-fat milk powder in tris buffered saline with 0.1% tween (TBS-T)[12] for 1 hour. Incubation with the primary antibodies was done at 4°C, overnight, followed by 40 minutes at room temperature. The primary antibodies used were mouse anti-EAAT1 (1:1000, Santa Cruz Biotechnology, sc-515839), mouse anti-EAAT2 (1:1000, Santa Cruz Biotechnology, sc-365634), or rabbit anti-GDNF (1:1000, Santa Cruz Biotechnology, sc-328). Mouse anti-glyceraldehyde-3-phosphate dehydrogenase (GAPDH) (1:5000, Sigma-Aldrich, MAB374) and mouse anti-tubulin (1:5000, Sigma-Aldrich, T9026) antibodies were incubated for 90 minutes at room temperature and were used for protein loading control. Goat anti-mouse IgG coupled to horseradish peroxidase (HRP) (1:20000, Santa Cruz Biotechnology, sc-2005) and goat anti-rabbit HRP (1:20000, Santa Cruz Biotechnology, sc-2004) were used as secondary antibodies, and were incubated during 1 hour at room temperature. Protein bands were visualized by enhanced chemiluminescence (ChemiDoc, Bio-Rad Laboratories) after incubation with Millipore Immobilon Crescendo Western HRP Substrate (Millipore, Cat: WBLUR0500) for 5 minutes. The densitometric analysis of each band was done with the ImageLab software (Bio-Rad Laboratories), and bands of the proteins of interest were normalized to the density of the band of the respective housekeeping protein.

---

[7] **Loading buffer:** 100 mM Tris (Fisher Scientific, M-27435), 100 mM Glycine (Fisher Scientific, BP381-1), 139 mM SDS (Panreac, 142363.1211), 8 M Urea (Acros, 140750010), 1.46 x 10^{-4} mM Bromophenol blue (Amresco, 0449), and 1.42 M β-mercaptoethanol (Merck, 8.05740.1000).

[8] **Stacking gel:** 531 mM acrylamide 30% (Panreac, A3626,0500), 124 mM Tris 0.5M, pH=6.8 (Fisher Scientific, M-27435), 3.45 mM SDS (Panreac, 142363.1211), 11.35 mM PSA (Panreac, 131138.1610), and 6.58 mM TEMED (Acros, 138455000).

[9] **Resolving gel:** 1.64 M acrylamide 30% (Panreac, A3626,0500), 373 mM Tris 1.5M, pH=8.8 (Fisher Scientific, M-27435), 3.45 mM SDS (Panreac, 142363.1211), 11.35 mM PSA (Panreac, 131138.1610), and 3.29 mM TEMED (Acros, 138455000).

[10] **Running buffer:** 25 mM Tris (Fisher Scientific, M-27435), 192 mM glycine (Fisher Scientific, BP381-1), and 3.45 mM SDS (Panreac, 142363.1211).

[11] **Transfer buffer:** 25 mM Tris (Fisher Scientific, M-27435), 192 mM glycine (Fisher Scientific, BP381-1), 0.173 mM SDS (Panreac, 142363.1211), and 10% methanol (Fisher Chemical, M/4000/17).

[12] **Tris Buffered Saline with 0.1% Tween (TBS-T):** 20 mM Tris (Fisher Scientific, M-27435), 140 mM NaCl (Fisher Scientific, S271-500), and 2.1.x 10-3 mM Tween 20 (Fisher Scientific, BP337-500).

3.6. Growth Factor Array

Analysis of growth factors present in the CM of the primary cultures of astrocytes was performed with RayBio® C-Series Rat Growth Factor Array 1 (AAR-GF-1-8) following the manufacturer's instructions. The growth factors analyzed in this array were BDNF, CSF2, EGF, FGF2, FLT3LG, GDNF, HGF, IGF1, IGFBP5, INHBA, NGF, PDGFA, PDGFB, and VEGFA. Briefly, the CM was centrifuged at 19280 g for 3 minutes to remove cell debris, and a pool was made with six samples from each experimental condition, making up to 1 ml. The samples were incubated for 5 hours at room temperature and the biotinylated antibody and HRP-Streptavidin was incubated for 2 hours at room temperature. The growth factor profile was performed in duplicate, and dots were detected using a chemiluminescence system (ChemiDoc, Bio-Rad Laboratories). Basically, one plastic sheet was placed on the detection system and the membrane was placed on top, followed by the detection buffers. The detection buffer was left on the membrane for 2 minutes, after which time another plastic sheet was placed, waited 15s, and detection was started. The calculated average pixel density of each pair of dots, representing relative levels of growth factors, was analyzed with ImageLab software. All the solutions used were included in the RayBio kit.

3.7. Polymerase Chain Reaction

To optimize the protocol for optimal annealing temperature and sample amount, a polymerase chain reaction (PCR) was performed. The primers for both GDNF and Cyclophilin A (CiA) (housekeeping) were designed with the Primer Blast-NCBI-NIH program after literature consultation and were purchased from STAB VIDA: CiA Fw 5'-CAA GAC TGA GTG GCT GGA TGG-3', Rv 5'- GCC CGC AAG TCA AAG AAA TTA GAG-3' fragment size 163 bp and GDNF Fw 5'- ACG AAA CCA AGG AGG AAC TGA - 3', Rv 5'-TTT GTC GTA CAT TGT CTC GGC -3' fragment size 74 bp.

For PCR, two mixes were prepared, one for CiA and one for GDNF. Each mix contained 2.5µl of 10x buffer, which already includes 20mM $MgCl_2$ (10X Dream Taq Buffer, EP0702, Fermentas), 0.5µl of dNTPs mix (100mM dATP - R0141, 100mM dCTP - R0151, 100mM dGTP - R0161, and 100mM dTTP - R0171, Thermo Scientific), 0.075µl forward primer, 0.075µl reverse primer, 0.625µl Taq (Dream Taq DNA polymerase, EP0702, Fermentas) and nuclease-free water (R0581, Fermentas) up to a total volume of 23µl in each condition. To determine which annealing temperature was most effective, 6 temperatures were tested (52, 54, 56, 58, 60, and 62°C). The T100 Thermal Cycler (BIO-RAD) was used for the reaction with the following protocol: 95°C for 3 minutes, followed by 40 cycles of 95°C for 30 seconds, then 45 seconds at the annealing

temperature (52, 54, 56, 58, 60, and 62°C), 1 minute at 72°C and finally 5 minutes at 72°C.

For visualization of the results, the PCR products were mixed with a 6X loading buffer (MB13101, Nzytech) and were subjected to electrophoresis on a 2% agarose gel for 1 hour at 130V with 0.003% GreenSafe (MB13201, Nzytech) and a ladder (NZYDNA Ladder VI, MB08901, Nzytech). The bands were visualized on a fluorescence gel imaging system (UVITEC Cambridge). The annealing temperature of 58°C achieved the best amplification for the GDNF primers (Figure 5.a) and CiA also achieved amplification at this temperature (Figure 5.b), so this temperature was chosen as the optimal annealing temperature.

a. **b.**

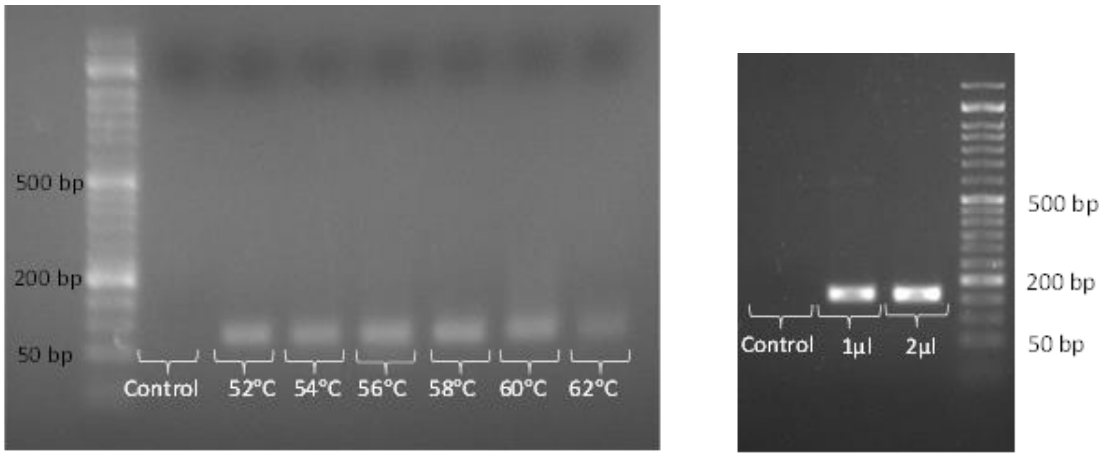

Figure 5 Representative image of the product obtained from conventional PCR. (**a**) Representative image of Gdnf mRNA. From left to right is represented the molecular weight ladder and seven bands. The first band is the negative control, and the next six bands represented the temperatures tested using 2µl cDNA. (**b**) Representative image of Cyclophilin A mRNA. From left to right is represented the negative control, two bands with 1µl and 2µl cDNA resultant form a protocol with an annealing temperature of 58°C, and the molecular weight ladder.

3.8. Reverse Transcription Polymerase Chain Reaction

To evaluate the efficiency of the primers and GDNF gene expression in the samples, a Reverse Transcription Polymerase Chain Reaction (RT-PCR) was performed. Primer efficiency was evaluated using various dilutions of the same sample (1:1; 1:5; 1:25; 1:125), and the efficiency of both primers was proved, CiA with 92.77% efficiency and GDNF with 107.63% efficiency. Two mixes were made, one for CiA and one for GDNF. Each mix contained 10µl of SYBR Green (Luminaris HiGreen Fluorescein qPCR Master Mix, K0981, Thermo Scientific), 0.06µl forward primer, 0.06µl reverse primer, the sample, and nuclease-free water until a total volume of 20µl, in which 4µl of the sample was used for the GDNF mix and 1µl of sample was used for the CiA mix. All samples were

run in duplicate. The following protocol was used in a CFX Connect Real-Time System (BIO-RAD): initial denaturation at 95°C for 10 minutes, denaturation at 95°C for 15 seconds, annealing at 58°C for 1 minute, extension at 72°C for 10 seconds (40 cycles) and finally 81 cycles of 10 seconds between 55°C and 95°C (0.5°C/cycle). Quantification was determined using cycle time (CT) values and after normalization to the housekeeping gene (CiA). The results were expressed as $2^{-\Delta\Delta CT}$ normalized to the control.

3.9. Neutralization of GDNF

To investigate the role of GDNF present in the CM of astrocytes, anti-GDNF (0.4 µg / ml, Santa Cruz, Cat: sc-328) was added to the medium for 20 minutes at room temperature. After this time, the CM was added to mixed cultures of astrocytes and neurons.

3.10. Immunocytochemistry

For the immunocytochemistry assays, the neuron-glial primary culture was grown in 24-well plates containing 13mm coverslips coated with PDL. On the 9th DIV, the cells were fixed with 4% paraformaldehyde in PBS (Acros, 169650010) for 10 minutes and washed with cold PBS. Then, a permeabilization solution (PBS with 1% Triton) was added for 10 minutes, and then, a blocking solution to reduce non-specific binding. For the immunocytochemistry of anti-MAP, a blocking solution with PBS 0.1% Tween and 20% FBS was added for 1 hour, and for the immunocytochemistry of anti-c-FOS, a blocking solution with PBS 0.1% Tween, 20% FBS, and 3% Bovine Serum Albumin) was added for 2 hours. After the blocking period, the primary antibodies used were rabbit anti-MAP (1:500, Santa Cruz Biotechnology, sc-20172), incubated overnight at 4°C, and mouse anti-c-FOS (1:100, Santa Cruz Biotechnology, sc-271243), incubated for 24 hours at 4°C. After a washing step with PBS-T, to remove unbound antibodies, the cells were incubated with the following secondary antibodies for 2 hours at room temperature: goat anti-rabbit (1:1000, Invitrogen, A11010, A546) and goat anti-mouse (1:1000, Invitrogen, A11001, A488). Next, coverslips were washed with PBS-T, incubated with Hoechst 33342 (1:1000, Invitrogen, H3569) for 10 minutes, washed with PBS-T, and finally the coverslips were mounted on microscope slides using DAKO (CS703) mounting medium. All antibodies and Hoechst 33342 were diluted in PBS-T with 1% FBS. The images were acquired on an epifluorescence microscope AxioObserver Z1 with an AxioCamMR3 camera and EC Plan-Neofluar 40×/1.3 Oil DIC M27 lens. Acquisition and processing of images were made with the AxioVision software (Carl Zeiss MicroImaging GmbH, version: 4.8.2.0).

3.11. Assay of cell viability

On the 9th DIV, the culture medium of neuron-glial cultures was aspirated and incubated with 200µl of MTT solution (0.5mg/mL, M2128-5G, Sigma-Aldrich) prepared in HBSS with glucose for 1 hour. The MTT solution was then collected, 200µl of 0.04M HCl in isopropanol was added, homogenized until the precipitate dissolved, and the absorbance was read on a 96-well plate at 570nm, using the 620nm reference filter.

3.12. Morphometric analysis of neurons

The morphometric analysis of neurons was realized in three independent cellular preparations. Two coverslips per experimental condition were used in each preparation, and fifteen neurons per coverslip were analyzed. The results are expressed as the mean neurite number per neuron and the mean neurite length per neuron.

Sholl analysis was done on each skeletonized neuron considering the soma of the cell as the origin. This analysis was executed with the FIJI software (v. 1.53q) using the plugin Simple Neurite Tracer, with a sphere separation of 5µm and without normalization. The results are expressed as the mean number of intersections per neuron. The area under the curve for the Sholl analysis was calculated using GraphPad Prism 8 (GraphPad Software Inc., San Diego, CA).

3.13. Cell counting

The number of cells expressing c-Fos was evaluated by immunocytochemistry. To assess the number of neurons expressing c-Fos, the number of cells labeled for this marker was counted and normalized to the number of Hoechst 33342 labeled cells. For the analysis, 2 coverslips and 15 fields per coverslip, were analyzed for each experimental condition. For each coverslip, the cells co-labeled were counted and normalized to the total of cells per field. The results are expressed as a percentage of control and represent the mean of three independent experiments (performed with independent cell cultures).

3.14. Statistical analysis

The results are expressed as specified in the text and figure legends. Each experimental condition was always performed in duplicate or triplicate in at least three different cellular preparations. Comparisons between three or more groups with only one variable were made with one-way ANOVA followed by Bonferroni's multiple comparison test, as indicated in the figure legends. Data are presented as mean ± standard error of the mean (SEM). Values of $P<0.05$ were considered significant. All statistical analyses were performed using GraphPad Prism 8 (GraphPad Software Inc., San Diego, CA).

Chapter 4

Results

4. Results

4.1. Effect of HF-rMS on the levels of glutamate transporters

Astrocytes are the main cells responsible for the removal of glutamate from the synaptic cleft [29]. This is accomplished through Na^+ and K^+ dependent glutamate transporters such as EAAT1 and EAAT2.

Previous studies realized by our group showed that astrocytes have an important role in HF-rMS mediated neuroprotection. Since excitotoxicity is a major cause of neuronal death, we proposed to evaluate whether the protection exerted by HF-rMS involved the regulation of glutamate transporters in astrocytes. To evaluate this hypothesis we determined, by Western Blot, the levels of the glutamate transporters EAAT1 and EAAT2 in astrocyte extracts. Two bands were observed for EAAT1, as shown in Figure 6.a, a monomer, and a dimer, with the dimer corresponding to the glycosylated form of EAAT1. This glycosylation of EAAT1 has been correlated with the passage of this transporter to the plasma membrane leading to an increased capacity for glutamate uptake [101]. The two bands formed for EAAT1 were evaluated separately. Although the quantification for the EAAT1 monomer showed no significant difference between the experimental conditions (Figure 6.b), the quantification for the EAAT1 dimer showed an increase of 51.3% from the OGD+HF-rMS experimental group when compared with the control ($P<0.01$; Figure 6.c). This means that when HF-rMS was performed on the cultures of astrocytes that had undergone OGD, there was an increase in the number of glycosylated glutamate transporters. Interestingly, in the group that underwent HF-rMS without having previously undergone OGD, there is no significant difference in the number of transporters, indicating that HF-rMS needs an initial stimulus to trigger the increase in the number of glutamate transporters.

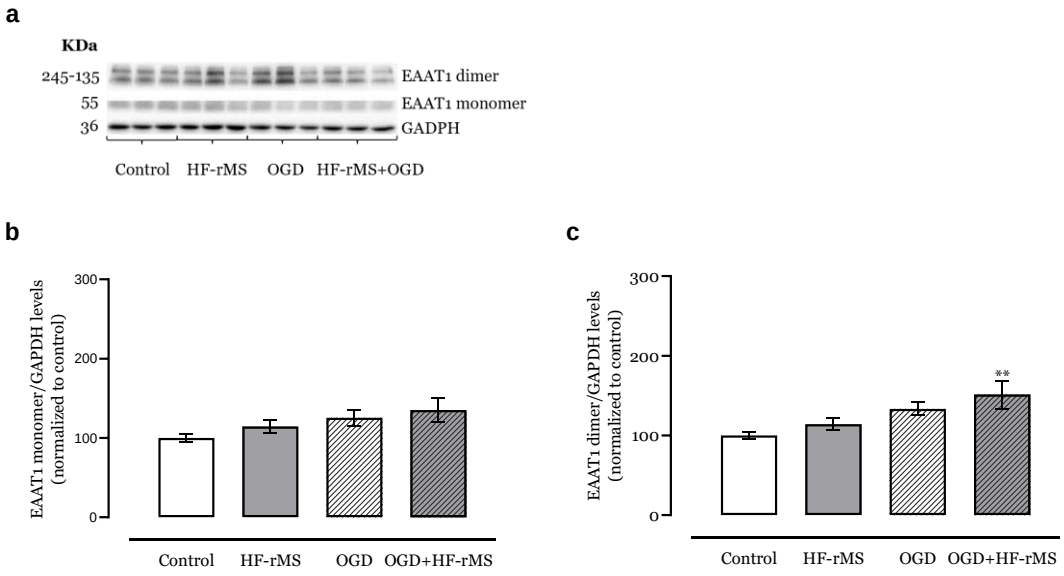

Figure 6 Effect of HF-rMS on glutamate transporter EAAT1 levels. Representative Western Blot bands for EAAT1 dimer (245-135KDa), EAAT1 monomer (55KDa), and GAPDH (36KDa) (**a**). Quantification of EAAT1 monomer normalized to GAPDH and to control (**b**). Quantification of EAAT1 dimer normalized to GAPDH and to control (**c**). Data is shown as mean ± SEM of six independent experiments performed in duplicate or triplicate. Statistical analysis was performed using one-way ANOVA followed by Bonferroni´s multiple comparisons tests (** P<0.01 to control; Supplementary Table 2).

One band, corresponding to a dimer was observed for EAAT2 (Figure 7.a). Quantification of this isoform, showed that there is no difference in the intensity of this band between the experimental groups (Figure 7.b), indicating that HF-rMS does not modulate the levels of this isoform of glutamate transporters.

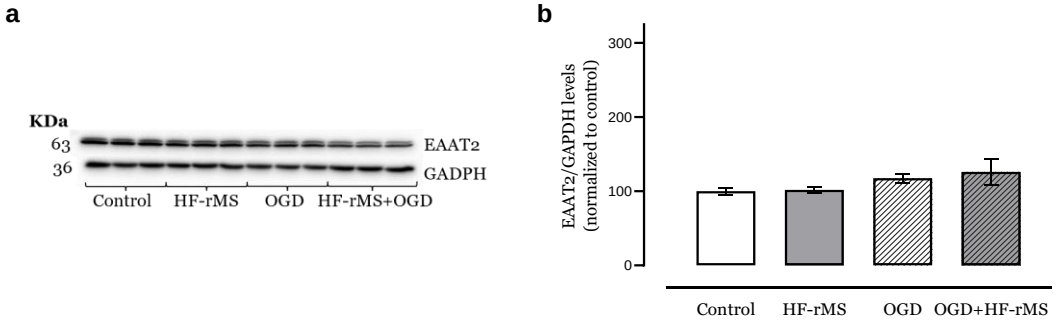

Figure 7 Effect of HF-rMS on glutamate transporter EAAT2 levels. Representative Western Blot bands for EAAT2 (63KDa), and GAPDH (36KDa) (**a**). Quantification of EAAT1 monomer normalized to GAPDH and to control (**b**). Data is shown as mean ± SEM of six independent experiments performed in duplicate or triplicate. Statistical analysis was performed using one-way ANOVA followed by Bonferroni´s multiple comparisons test (Supplementary Table 2).

4.2. Effects of HF-rMS on the levels of growth factors present in the culture medium

Previous studies from our group demonstrated that the medium conditioned by astrocytes that had undergone OGD and HF-rMS to neuron cultures promoted neuroprotection, showing that astrocytes release factors that are crucial to the HF-rMS-mediated neuroprotection. Since a widely documented way for astrocytes to promote neuroprotection is through the secretion of neurotrophic factors [37, 102], a panel of neurotrophic factors and how their levels were affected by OGD and HF-rMS was evaluated. For this, astrocyte-enriched cultures were exposed to HF-rMS, and the growth factors present levels in the culture medium were analyzed using an antibody array (Figure 8).

4.2.1. HF-rMS modulates the release of growth factors by astrocytes

As previously mentioned, astrocyte-CM prevents ischemia-induced neurite degeneration. To identify which growth factors are involved in this effect triggered by HF-rMS, astrocyte-enriched cultures (control and OGD) were exposed to HF-rMS, and the growth factors present in the culture medium were analyzed using a semi-quantitative antibody array. Of the fourteen growth factors analyzed, six of them showed an increase in one of the groups that were subjected to HF-rMS. Activin A which showed an increase in the HF-rMS group, FLT3 ligand presented an increase in the OGD+HF-rMS group, and bFGF and VEGF-A presented increase levels in both HF-rMS and OGD groups (Figure 8). Both GDNF and PDGF-BB show an increase over control and OGD in both HF-rMS and OGD + HF-rMS group.

GDNF is a neurotrophic factor that promotes survival and differentiation of neurons and was shown to have the ability to reduce the infarct zone and brain edema after IS, is related to anti-apoptotic properties, and affects neurogenesis after stroke [37]. To determine whether HF-rMS altered Gdnf mRNA and GDNF protein levels a Western Blot and a RT-PCR was performed on cell extracts collected from astrocyte-enriched cultures.

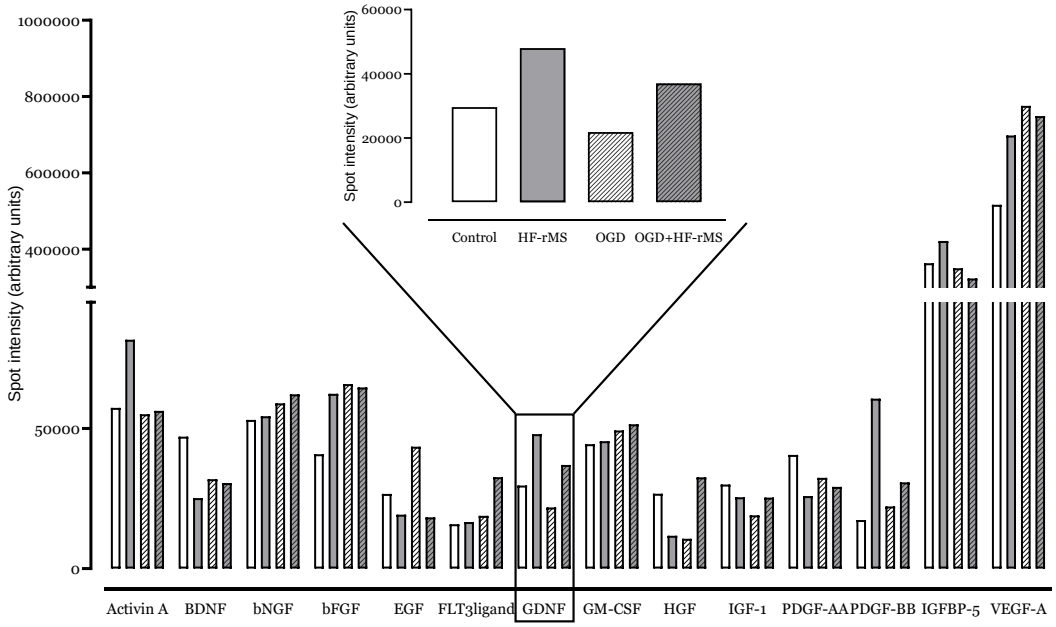

Figure 8 Effect of HF-rMS in growth factor levels present in the CM from astrocyte-enriched cultures exposed to OGD. Semi-quantitative detection of fourteen growth factors using an antibody array, with a focus on GDNF. Each bar corresponds to the average value of two pools of six samples each, performed in duplicate.

4.2.2. HF-rMS induces GDNF expression in a cellular model of ischemia

Exposure to HF-rMS after OGD increased Gdnf mRNA levels on astrocyte-enriched cultures by approximately 126.3% (Figure 9.c). In the absence of OGD, HF-rMS was unable to promote the expression of Gdnf mRNA levels. Similarly, quantification of GDNF protein (Figure 9.a.), showed that astrocyte-enriched cultures exposed to OGD and treated with HF-rMS presented an increase of GDNF protein levels of 66.8% (Figure 9.b). In the absence of OGD, HF-rMS was unable to promote an increase of GDNF protein. HF-rMS alone was able to induce GDNF release, whereas upregulation of GDNF mRNA and protein levels was only observed in cultures previously exposed to OGD suggesting a differential effect of HF-rMS on healthy and injured cells, and different regulation of gene expression and mechanisms of release.

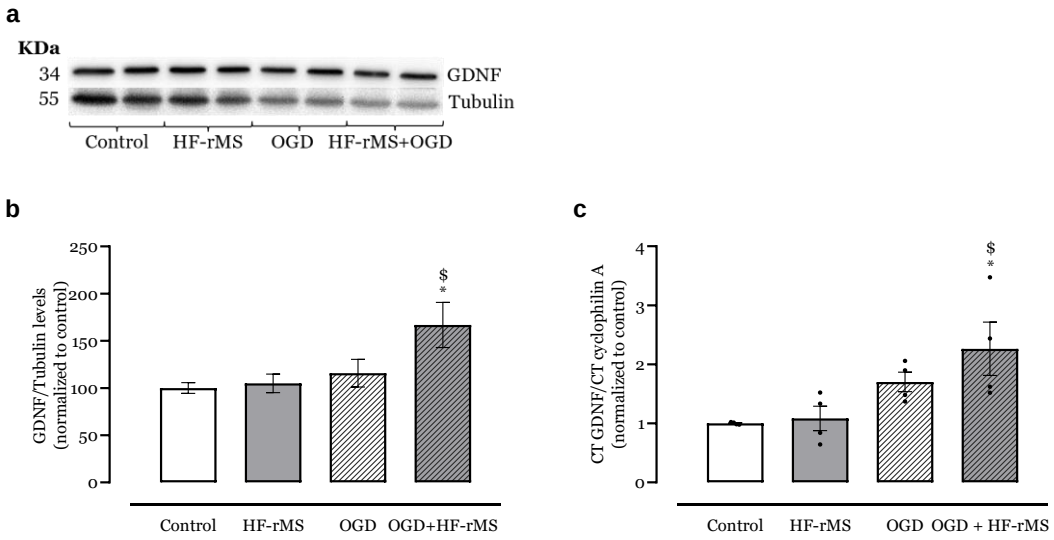

Figure 9 GDNF levels in astrocyte-enriched cultures subjected to OGD and HF-rMS. Representative Western Blot bands for GDNF (34KDa), and Tubulin (55KDa) are shown (**a**). Quantification of GDNF normalized to Tubulin and to control. Data is shown as mean ± SEM of three independent experiences performed in duplicate (**b**). Quantification of the Gdnf mRNA levels in astrocyte-enriched cultures. Data is shown as mean ± SEM of four independent experiments, each represented by a dot (**c**). Statistical analysis was performed using one-way ANOVA followed by Bonferroni´s multiple comparisons tests (* P<0.05 to control, $ P<0.05 to HF-rMS; Supplementary Table 2).

4.2.3. GDNF neutralization does not interfere with cell viability after HF-rMS

To evaluate the participation of GDNF in the neuroprotection induced by HF-rMS the cell viability the MTT assay was used. As expected, there was a significant decrease of cell viability in OGD-exposed cells (P<0.001), however, this effect was not altered by HF-rMS or GDNF neutralization (Figure 10). These data agree with previous data from our group showing that HF-rMS does not improve cell viability, but rather protects, and enhances the function of the survival neurons.

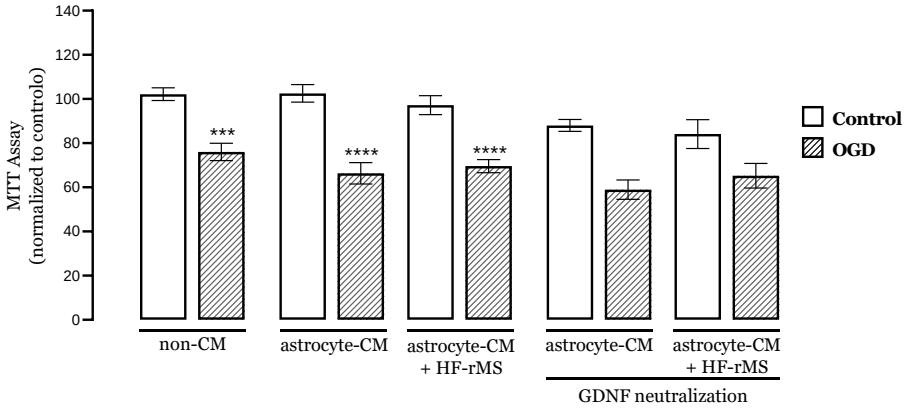

Figure 10 Effects of neutralizing the GDNF present in astrocyte-CM on cell viability. The absorbance values of experimental conditions were normalized to the values of non-CM condition. All results represent the mean ± SEM from six independent cell preparations with each experimental condition performed in triplicate. Statistical analysis was performed using one-way ANOVA followed by Bonferroni's multiple comparisons tests (***P<0.001, ****P<0.0001 compared to non-CM; Supplementary Table 2).

4.2.4. GDNF neutralization blocks the recovery of neurite number and length induced by HF-rMS

GDNF present in the CM from astrocyte-enriched cultures was neutralized, using a specific antibody, before its transference to neuron-glial cortical cultures, and the number of neurites, its length, and neuronal arborization was assessed (Figure 11). As expected, the ischemic insult led to a decrease in the number of neurites (from 7.867±0.3925 to 5.222±0.3053 μm; Figure 11.a), on neurite length (from 48.24±1.603 to 30.16±1.531 μm; Figure 11.b), and in neuronal arborization (Figure 11.c and 11.d). The results also indicated that the CM from control astrocyte-CM did not prevent ischemia-induced neurite degeneration. However, CM from astrocyte-enriched cultures exposed to HF-rMS increased the number of neurites (from 7.867±0.3925 to 9.978±0.6778 μm; Figure 11.a), the length of the neurites (from 48.24±1.603 to 70.43±4.742 μm; Figure 11.b), and neuronal arborization (Figure 11.c and 11.d). A similar effect occurred when the neuron-glial culture was previously subjected to OGD. The CM from astrocyte-enriched cultures exposed to HF-rMS increased the number of neurites (from 5.222±0.3053 to 9.8±0.6489 μm; Figure 11.a), the length of the neurites (from 30.16±1.531 to 60.10±1.418 μm; Figure 11.b), and neuronal arborization (Figure 11.c and 11.d) in OGD exposed cultures. However, the neutralization of the GDNF present in the CM led to the complete loss of the protective effects induced by HF-rMS. Neutralization of GDNF in CM from astrocyte-enriched cultures exposed to HF-rMS decreased the number of neurites (from 9.978±0.6778 to 5.167±0.3859 μm; Figure 11.a), the length of the neurites (from 70.43±4.842 to 36.68±3.496 μm; Figure 11.b), and neuronal arborization (Figure 11.c and 11.d). A similar effect occurred in neuron-glial cultures subjected to OGD. The neutralization of GDNF in the CM from astrocyte-enriched cultures exposed to HF-rMS decreased the number of neurites (from 9.8±0.6489 to 5.144±0.5991 μm; Figure 11.a), the length of the neurites (from 60.10±2.418 to 29.71±4.344 μm; Figure 11.b), and neuronal arborization (Figure 11.c and 11.d) in OGD exposed cultures. These data suggest that the GDNF released into the medium significantly contributes to the neuroprotection triggered by HF-rMS after OGD.

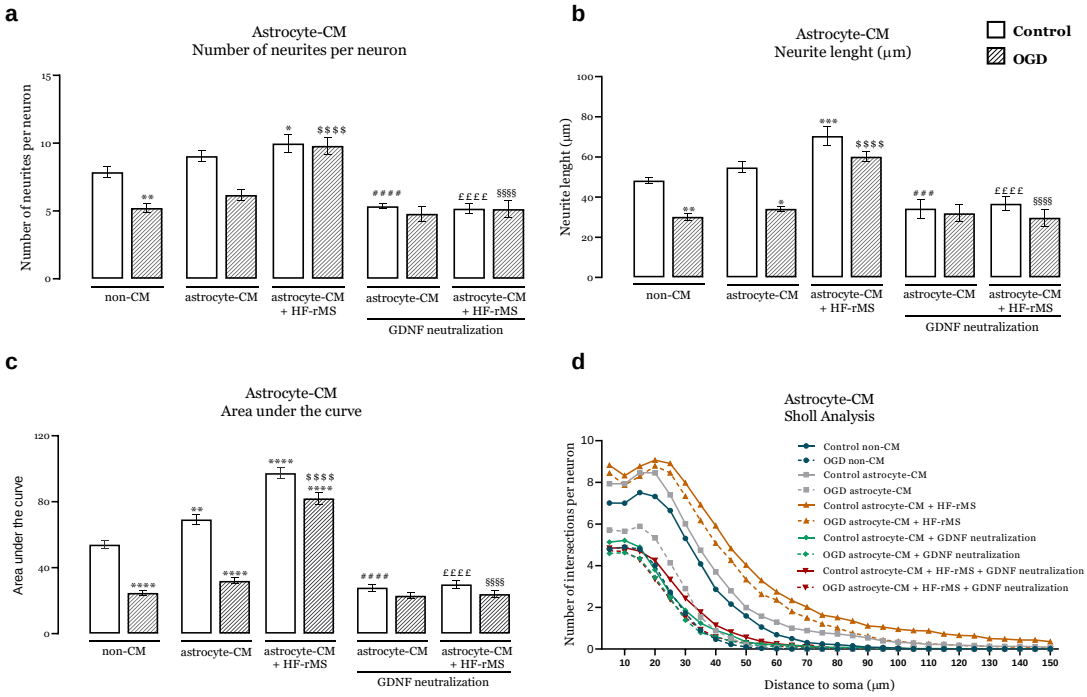

Figure 11 Effects of neutralizing the GDNF present in the astrocyte-CM on ischemia-induced neurite degeneration. Quantification of the number of neurites per neuron (**a**), neurite length (**b**), area under the curve from Sholl analysis (**c**), and the number of intersections per neuron on the distance to the soma (**d**). All results represent the mean ± SEM from three independent cell preparations with each experimental condition performed in duplicate. Statistical analysis was performed using one-way ANOVA followed by Bonferroni's multiple comparisons test (*P<0.05, **P<0.01, ***P<0.001, ****P<0.0001 compared to Control non-CM; ###P<0.001, ####P<0.0001 compared to Control astrocyte-CM; £££££P<0.0001 compared to Control astrocyte-CM + HF-rMS; $$$$P<0.0001 compared to OGD astrocyte-CM, and §§§§P<0.0001 compared to OGD astrocyte-CM + HF-rMS; Supplementary Table 2).

4.2.5. GDNF neutralization blocks the increased in the number of neurons expressing c-Fos induced by HF-rMS after ischemia

To further characterize the role of GDNF released by HF-rMS-exposed astrocytes to the neuroprotection achieved, the number of cells expressing c-Fos, a molecular marker of neuronal activity, was assessed by immunocytochemistry (Figure 12). As expected, in neuron-glial cultures OGD induced a decrease of 38.7% in the number of cells labeled for c-Fos (Figure 12). On the other hand, CM from astrocyte cultures exposed to HF-rMS increased the number of cells expressing c-Fos by 79.6%, and a similar effect occurred in neuron-glial cultures subjected to OGD. The CM from astrocyte cultures exposed to HF-rMS increased the number of cells expressing c-Fos in OGD-exposed cultures by 112.6%. Interestingly, neutralization of GDNF in CM from astrocyte cultures exposed to HF-rMS completely inhibited the effect triggered by HF-rMS in neuron-glial cultures subjected to OGD, decreasing the number of cells expressing c-Fos by 115.9%. Similarly, in control conditions, neutralization of GDNF in CM from astrocyte cultures exposed to HF-rMS decreased the number of cells expressing c-Fos by 124.2%.

These data suggest that the GDNF released into the medium significantly contributes to the neuroprotection triggered by HF-rMS in OGD-injured cultures.

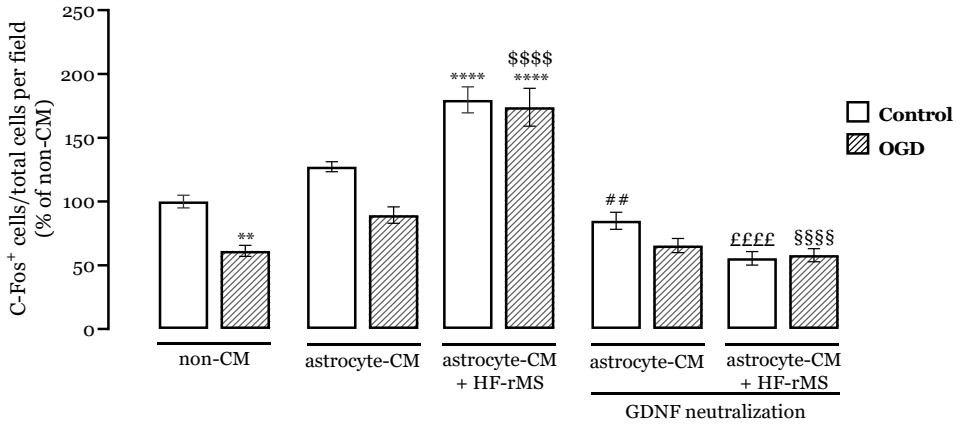

Figure 12 Neutralization of GDNF present in the CM from HF-rMS-exposed astrocytes impedes the recovery in the number of neurons expressing c-Fos. Results are expressed as a percentage of non-CM and represent the mean ± SEM from three independent cell preparations, each experimental condition performed in duplicate. Statistical analysis was performed using one-way ANOVA followed by Bonferroni's multiple comparisons tests (**P<0.01, ****P<0.0001 compared to Control non-CM; ##P<0.01 compared to Control astrocyte-CM; £££££P<0.0001 compared to Control astrocyte-CM + HF-rMS; $$$$P<0.0001 compared to OGD astrocyte-CM, and §§§§P<0.0001 compared to OGD astrocyte-CM + HF-rMS; Supplementary Table 2).

Chapter 5

Discussion

5. Discussion

Increasing data from clinical trials demonstrated the benefits of HF-rMS in ameliorating the impairments of several neurologic and neuropsychiatric disorders. IS is one of the conditions in which this therapy has been shown to improve the most common deficits such as dysphagia, aphasia, hemispatial neglect, depression, and cognitive deficits [43-45]. rTMS is highly associated with neuronal plasticity [52, 53]. Despite HF-rTMS being applied to patients and demonstrating beneficial results, the biological mechanisms behind its effect are not fully understood. The existing studies focus mainly on the effects of rTMS on neurons and the identified effects are increased ATP and glucose metabolism [103], prevention of neuronal death [89, 104], reduced infarct volume [103], increased neurogenesis [89], and neuroplasticity [105], hyperexcitability [106], modulation of gene expression [89], and increased synaptic plasticity [99]. However, some studies have also demonstrated the effects of HF-rMS on glial cells. Hong and colleagues (2020) observed a conversion from the A1 phenotype to the A2 phenotype after HF-rMS and, consequently, a decrease in astrocyte reactivity [82]. It was also observed that HF-rMS decrease inflammation by decreasing the levels of the pro-inflammatory mediator TNF-α, IL-1β, and TGF-β, and increasing the anti-inflammatory mediator IL-10 present in the cell medium [82, 89]. Besides these effects, HF-rTMS caused an upregulation of VEGF-A and VEGF-B, which promotes angiogenesis, that in turn protected capillary integrity, observed by an increase in CD31 positive cells [89, 98]. These data suggest that glial cells are crucial targets for the neuroprotection caused by HF-rTMS. A recent study from our group demonstrated that the application of HF-rTMS prevents neuronal death and neurite degeneration induced by OGD and increases the number of cells expressing ERK1/2 and c-Fos, and the number and intensity of synaptic puncta. Importantly, these effects were only observed in neuron-astrocyte cultures, and not in neuron-enriched cultures, thus suggesting that astrocytes are essential for the beneficial effects induced by HF-rMS after ischemia [99]. Subsequently, another work from our group showed that these beneficial effects occurred both in the presence of astrocytes and in the presence of their secretome alone [107].

Astrocytes are the most abundant cells in the central nervous system and play an important role in maintaining brain function. After an ischemic stroke, astrocytes have a neuroprotective effect due to the release of neurotrophic factors and the limitation of excitotoxicity [108]. In addition, astrocytes contribute to angiogenesis, neurogenesis, synaptogenesis, and axonal remodeling [109, 110]. Considering that excitotoxicity is one of the main factors leading to neuronal death and that astrocytes are the main cells responsible for decreasing excitotoxicity [108], we evaluated the effect of HF-rMS on the

levels of glutamate transporters EAAT1 and EAAT2 expressed by astrocytes. The glutamate transporters EAAT1 and EAAT2 are mainly expressed in astrocytes, although they may also be present in microglia and oligodendrocytes [111]. Western Blot analysis showed that EAAT2 levels were not affected by HF-rMS, however, EAAT1 levels increased in cultures subjected to OGD and HF-rMS, suggesting that HF-rMS promotes glutamate capture from the synaptic cleft. The action of HF-rMS on the levels of the glutamate transporter EAAT1 is context-dependent, as an increase in its levels only occurs when HF-rMS is applied to cells previously exposed to OGD. Several studies have already demonstrated the importance of these two transporters in *in vivo* models of IS. Delyfer and colleagues (2015) demonstrated that EAAT1 inhibition increased extracellular glutamate levels leading to neuronal death by excitotoxicity [112], but they also demonstrated the importance of EAAT2 in decreasing excitotoxicity. EAAT2 knockdown exacerbated neuronal damage, indicating that EAAT2-mediated glutamate uptake is essential for neuronal survival [113]. Furthermore, overexpression of EAAT2 showed that this transporter reduced excess glutamate levels, thereby decreasing ischemia-associated brain death [114]. The action of glutamate transporters after TMS has also been studied. The application of HF-rTMS in mice increased the levels of glutamate transporters (EAAT1 and EAAT2) in the absence of injury [115], and in rats, a single session of iTBS increases EAAT2 expression, which could indicate a greater efficiency in glutamate uptake leading to a reduction in excitatory transmission [116]. To the best of our knowledge, our study is the first to demonstrate an increase in EAAT1 levels after HF-rMS in an *in vitro* model of ischemia. However, it is important to assess the glutamate levels in the extracellular medium to know the real changes in EAAT1.

Furthermore, and given that our group has recently demonstrated that the secretome of astrocytes is important for the beneficial effects induced by HF-rMS [107], we evaluated what factors are released by astrocytes to the extracellular medium in response to HF-rMS, specifically which neurotrophic factors, since they are recognized as one of the ways astrocytes used to promote neuroprotection [37, 102]. Using a Growth Factor Array we evaluated 14 neurotrophic factors present in astrocytes-CM and observed an increase in GDNF and PDGF-BB in both groups subjected to HF-rMS. As GDNF is a neurotrophic factor that promotes survival and differentiation of neurons and has demonstrated anti-apoptotic properties and the ability to reduce the infarct area, and brain edema [37], we evaluated the expression of Gdnf mRNA levels by RT-PCR and GDNF protein levels by Western Blot after HF-rMS. An increase in both mRNA and protein expression was verified in the HF-rMS + OGD groups. To confirm the contribution of GDNF to the neuroprotective effects induced by the secretome of HF-rMS-exposed astrocytes the GDNF present in the CM was neutralized with a specific

antibody. This neutralization impeded the protective effects induced by HF-rMS, namely in preventing neurite degeneration and promoting neuronal activation, assessed by c-Fos labeling. Several studies have demonstrated the importance of GDNF liberated by astrocytes to induce neuroprotection after IS. In IS models, GDNF has shown the capacity to reduce apoptosis [117], reduce excitotoxicity by increasing EAAT1 and EAAT2 levels [118-120], lower the calcium influx induced by overactivation of NMDA receptors [121] and reduce oxidative stress [122]. Moreover, GDNF promotes peri-infarct brain remodeling and contralesional neuroplasticity [123]. The neuroprotective actions triggered by neurotrophic factors released by HF-rTMS, namely BDGF, GDNF, b-NGF, PDGF-AA, VEGF, and NT-3, were also shown [124-127]. Nevertheless, the ability of HF-rTMS to modulate the levels of GDNF was only demonstrated in animal models of Parkinson´s disease and neuroblastoma cultures [124-126]. Therefore, to the best of our knowledge, our study is the first to demonstrate the capacity of HF-rMS to modulate the release of GDNF, and more importantly, that the release of GDNF by astrocytes, plays a crucial role in neuronal protection mediated by HF-rMS.

Taken together, our results show that HF-rTMS may be a valuable therapeutic approach as it directly modulates astrocytes by increasing the levels of glutamate transporters, which consequently may lead to decreased excitotoxicity. HF-rMS also triggers the release of mediators, specifically neurotrophic growth factor GDNF, that will promote neuronal survival after a period of ischemia. It is already known that neuronal activity affects astrocyte function and, conversely, astrocytes are key cellular components in the regulation of synapses, namely by releasing factors that regulate the number of synapses formed [128]. Our results show that the neuronal survival observed after HF-rMS involves astrocytes. However, the effect of TMS on astrocytes are likely to be influenced by the presence of other cell types and the conditions of these cells. Therefore, to clarify the influence of other cell types on what was observed in the present study, it would be important to evaluate the effects of TMS on astrocytes when cultured with other cell types, namely microglia and oligodendrocytes. Our results may be an important step in understanding how the brain responds to HF-rTMS after ischemic injury, at the cellular and molecular level, thus leading to the faster implementation of HF-rTMS as a therapeutic approach in ischemic stroke recovery.

Chapter 6

Conclusions and Future Perspectives

6.Conclusions and Future Perspectives

Through this work, we explored the mechanisms triggered by HF-rMS in astrocytes that contribute to their neuroprotective action. The data obtained showed that HF-rMS has a direct modulatory effect on astrocytes increasing the glutamate transporter EAAT1, which may suggest its role in reducing excitotoxicity, and that it also affects the expression and release of chemical mediators to the medium, namely the release of neurotrophic factors, such as GDNF, which contributes to the promotion of neuroprotection in ischemia.

However, further experiments could be done to better understand the effects of HF-rMS on non-neuronal cells that contribute to its neuroprotective effects in brain ischemia:

- Analyze whether the observed increase in EAAT1 levels translates into a decrease in extracellular glutamate levels. For this, we could measure glutamate levels in the extracellular medium (e.g., by ELISA).
- Evaluate if HF-rMS affects other glial cells, such as microglia, cells essential in the neuroinflammatory process occurring in ischemic stroke, and whether a putative effect may contribute to the benefits of HF-rMS. For this, we could implement cultures of neurons, astrocytes, and microglia, and analyze markers of microglial reactivity (e.g., Iba-1, CD68, Arg-1).
- Analyze the impact of different rMS protocols on astrocytes, to evaluate if other protocols could potentiate the neuroprotective effects after an ischemic insult.
- Implement the MCAO model to evaluate the impact of HF-rTMS *in vivo*, and assess the effects on different non-neuronal components, maintaining the interactions that occur in the body and are lost in *in vitro* studies.

Chapter 7

Bibliographic References

7. Bibliographic References

1. Donkor ES. Stroke in the 21(st) Century: A Snapshot of the Burden, Epidemiology, and Quality of Life. Stroke Res Treat. 2018;2018:3238165. https://doi.org/10.1155/2018/3238165

2. Powers WJ, Rabinstein AA, Ackerson T, Adeoye OM, Bambakidis NC, Becker K, Biller J, Brown M, Demaerschalk BM, Hoh B, et al. Guidelines for the Early Management of Patients With Acute Ischemic Stroke: 2019 Update to the 2018 Guidelines for the Early Management of Acute Ischemic Stroke: A Guideline for Healthcare Professionals From the American Heart Association/American Stroke Association. Stroke. 2019;50(12):e344-e418. https://doi.org/10.1161/str.0000000000000211

3. Feigin VL, Nguyen G, Cercy K, Johnson CO, Alam T, Parmar PG, Abajobir AA, Abate KH, Abd-Allah F, Abejie AN, et al. Global, Regional, and Country-Specific Lifetime Risks of Stroke, 1990 and 2016. N Engl J Med. 2018;379(25):2429-37. https://doi.org/10.1056/NEJMoa1804492

4. Béjot Y, Bailly H, Durier J, Giroud M. Epidemiology of stroke in Europe and trends for the 21st century. Presse Med. 2016;45(12 Pt 2):e391-e8. https://doi.org/10.1016/j.lpm.2016.10.003

5. Freitas-Silva M, Medeiros R, Nunes JPL. Risk factors among stroke subtypes and its impact on the clinical outcome of patients of Northern Portugal under previous aspirin therapy. Clin Neurol Neurosurg. 2021;203:106564. https://doi.org/10.1016/j.clineuro.2021.106564

6. Radak D, Katsiki N, Resanovic I, Jovanovic A, Sudar-Milovanovic E, Zafirovic S, Mousad SA, Isenovic ER. Apoptosis and Acute Brain Ischemia in Ischemic Stroke. Curr Vasc Pharmacol. 2017;15(2):115-22. https://doi.org/10.2174/1570161115666161104095522

7. Feske SK. Ischemic Stroke. Am J Med. 2021;134(12):1457-64. https://doi.org/10.1016/j.amjmed.2021.07.027

8. Smith SD, Eskey CJ. Hemorrhagic stroke. Radiol Clin North Am. 2011;49(1):27-45. https://doi.org/10.1016/j.rcl.2010.07.011

9. Virani SS, Alonso A, Aparicio HJ, Benjamin EJ, Bittencourt MS, Callaway CW, Carson AP, Chamberlain AM, Cheng S, Delling FN, et al. Heart Disease and Stroke Statistics-2021 Update: A Report From the American Heart Association. Circulation. 2021;143(8):e254-e743. https://doi.org/10.1161/cir.0000000000000950

10. Raghavan P. Upper Limb Motor Impairment After Stroke. Phys Med Rehabil Clin N Am. 2015;26(4):599-610. https://doi.org/10.1016/j.pmr.2015.06.008

11. Benjamin EJ, Virani SS, Callaway CW, Chamberlain AM, Chang AR, Cheng S, Chiuve SE, Cushman M, Delling FN, Deo R, et al. Heart Disease and Stroke Statistics-2018 Update: A Report From the American Heart Association. Circulation. 2018;137(12):e67-e492. https://doi.org/10.1161/cir.0000000000000558

12. Jones CA, Colletti CM, Ding MC. Post-stroke Dysphagia: Recent Insights and Unanswered Questions. Curr Neurol Neurosci Rep. 2020;20(12):61. https://doi.org/10.1007/s11910-020-01081-z

13. Pula JH, Yuen CA. Eyes and stroke: the visual aspects of cerebrovascular disease. Stroke Vasc Neurol. 2017;2(4):210-20. https://doi.org/10.1136/svn-2017-000079

14. Kessner SS, Bingel U, Thomalla G. Somatosensory deficits after stroke: a scoping review. Top Stroke Rehabil. 2016;23(2):136-46. https://doi.org/10.1080/10749357.2015.1116822

15. Sun JH, Tan L, Yu JT. Post-stroke cognitive impairment: epidemiology, mechanisms and management. Ann Transl Med. 2014;2(8):80. https://doi.org/10.3978/j.issn.2305-5839.2014.08.05

16. Chohan SA, Venkatesh PK, How CH. Long-term complications of stroke and secondary prevention: an overview for primary care physicians. Singapore Med J. 2019;60(12):616-20. https://doi.org/10.11622/smedj.2019158

17. Meng G, Ma X, Li L, Tan Y, Liu X, Liu X, Zhao Y. Predictors of early-onset post-ischemic stroke depression: a cross-sectional study. BMC Neurol. 2017;17(1):199. https://doi.org/10.1186/s12883-017-0980-5

18. Chun HY, Whiteley WN, Dennis MS, Mead GE, Carson AJ. Anxiety After Stroke: The Importance of Subtyping. Stroke. 2018;49(3):556-64. https://doi.org/10.1161/strokeaha.117.020078

19. Rousselet E, Kriz J, Seidah NG. Mouse model of intraluminal MCAO: cerebral infarct evaluation by cresyl violet staining. J Vis Exp. 2012;(69) https://doi.org/10.3791/4038

20. Engel O, Kolodziej S, Dirnagl U, Prinz V. Modeling stroke in mice - middle cerebral artery occlusion with the filament model. J Vis Exp. 2011;(47) https://doi.org/10.3791/2423

21. Labat-gest V, Tomasi S. Photothrombotic ischemia: a minimally invasive and reproducible photochemical cortical lesion model for mouse stroke studies. J Vis Exp. 2013;(76) https://doi.org/10.3791/50370

22. Lunardi Baccetto S, Lehmann C. Microcirculatory Changes in Experimental Models of Stroke and CNS-Injury Induced Immunodepression. Int J Mol Sci. 2019;20(20) https://doi.org/10.3390/ijms20205184

23. Sommer CJ. Ischemic stroke: experimental models and reality. Acta Neuropathol. 2017;133(2):245-61. https://doi.org/10.1007/s00401-017-1667-0

24. Durukan A, Tatlisumak T. Acute ischemic stroke: overview of major experimental rodent models, pathophysiology, and therapy of focal cerebral ischemia. Pharmacol Biochem Behav. 2007;87(1):179-97. https://doi.org/10.1016/j.pbb.2007.04.015

25. Holloway PM, Gavins FN. Modeling Ischemic Stroke In Vitro: Status Quo and Future Perspectives. Stroke. 2016;47(2):561-9. https://doi.org/10.1161/strokeaha.115.011932

26. Steliga A, Kowiański P, Czuba E, Waśkow M, Moryś J, Lietzau G. Neurovascular Unit as a Source of Ischemic Stroke Biomarkers-Limitations of Experimental Studies and Perspectives for Clinical Application. Transl Stroke Res. 2020;11(4):553-79. https://doi.org/10.1007/s12975-019-00744-5

27. Lewerenz J, Maher P. Chronic Glutamate Toxicity in Neurodegenerative Diseases-What is the Evidence? Front Neurosci. 2015;9:469. https://doi.org/10.3389/fnins.2015.00469

28. Lee JM, Grabb MC, Zipfel GJ, Choi DW. Brain tissue responses to ischemia. J Clin Invest. 2000;106(6):723-31. https://doi.org/10.1172/jci11003

29. Hernández IH, Villa-González M, Martín G, Soto M, Pérez-Álvarez MJ. Glial Cells as Therapeutic Approaches in Brain Ischemia-Reperfusion Injury. Cells. 2021;10(7) https://doi.org/10.3390/cells10071639

30. Xu S, Lu J, Shao A, Zhang JH, Zhang J. Glial Cells: Role of the Immune Response in Ischemic Stroke. Front Immunol. 2020;11:294. https://doi.org/10.3389/fimmu.2020.00294

31. Qin C, Zhou LQ, Ma XT, Hu ZW, Yang S, Chen M, Bosco DB, Wu LJ, Tian DS. Dual Functions of Microglia in Ischemic Stroke. Neurosci Bull. 2019;35(5):921-33. https://doi.org/10.1007/s12264-019-00388-3

32. Meldrum BS. Glutamate as a neurotransmitter in the brain: review of physiology and pathology. J Nutr. 2000;130(4S Suppl):1007s-15s. https://doi.org/10.1093/jn/130.4.1007S

33. Sears SM, Hewett SJ. Influence of glutamate and GABA transport on brain excitatory/inhibitory balance. Exp Biol Med (Maywood). 2021;246(9):1069-83. https://doi.org/10.1177/1535370221989263

34. Farokhi-Sisakht F, Farhoudi M, Sadigh-Eteghad S, Mahmoudi J, Mohaddes G. Cognitive Rehabilitation Improves Ischemic Stroke-Induced Cognitive Impairment: Role of Growth Factors. J Stroke Cerebrovasc Dis. 2019;28(10):104299. https://doi.org/10.1016/j.jstrokecerebrovasdis.2019.07.015

35. Larpthaveesarp A, Ferriero DM, Gonzalez FF. Growth factors for the treatment of ischemic brain injury (growth factor treatment). Brain Sci. 2015;5(2):165-77. https://doi.org/10.3390/brainsci5020165

36. Rhim T, Lee M. Targeted delivery of growth factors in ischemic stroke animal models. Expert Opin Drug Deliv. 2016;13(5):709-23. https://doi.org/10.1517/17425247.2016.1144588

37. Lanfranconi S, Locatelli F, Corti S, Candelise L, Comi GP, Baron PL, Strazzer S, Bresolin N, Bersano A. Growth factors in ischemic stroke. J Cell Mol Med. 2011;15(8):1645-87. https://doi.org/10.1111/j.1582-4934.2009.00987.x

38. Rabinstein AA. Treatment of Acute Ischemic Stroke. Continuum (Minneap Minn). 2017;23(1, Cerebrovascular Disease):62-81. https://doi.org/10.1212/con.0000000000000420

39. Azad TD, Veeravagu A, Steinberg GK. Neurorestoration after stroke. Neurosurg Focus. 2016;40(5):E2. https://doi.org/10.3171/2016.2.focus15637

40. Bernardo-Castro S, Albino I, Barrera-Sandoval Á M, Tomatis F, Sousa JA, Martins E, Simões S, Lino MM, Ferreira L, Sargento-Freitas J. Therapeutic Nanoparticles for the Different Phases of Ischemic Stroke. Life (Basel). 2021;11(6) https://doi.org/10.3390/life11060482

41. Rikhtegar R, Yousefi M, Dolati S, Kasmaei HD, Charsouei S, Nouri M, Shakouri SK. Stem cell-based cell therapy for neuroprotection in stroke: A review. J Cell Biochem. 2019;120(6):8849-62. https://doi.org/10.1002/jcb.28207

42. Rajkovic O, Potjewyd G, Pinteaux E. Regenerative Medicine Therapies for Targeting Neuroinflammation After Stroke. Front Neurol. 2018;9:734. https://doi.org/10.3389/fneur.2018.00734

43. Lefaucheur JP, Aleman A, Baeken C, Benninger DH, Brunelin J, Di Lazzaro V, Filipović SR, Grefkes C, Hasan A, Hummel FC, et al. Evidence-based guidelines on the therapeutic use of repetitive transcranial magnetic stimulation (rTMS): An update (2014-2018). Clin Neurophysiol. 2020;131(2):474-528. https://doi.org/10.1016/j.clinph.2019.11.002

44. Dionísio A, Duarte IC, Patrício M, Castelo-Branco M. The Use of Repetitive Transcranial Magnetic Stimulation for Stroke Rehabilitation: A Systematic Review. J Stroke Cerebrovasc Dis. 2018;27(1):1-31. https://doi.org/10.1016/j.jstrokecerebrovasdis.2017.09.008

45. Kim WJ, Rosselin C, Amatya B, Hafezi P, Khan F. Repetitive transcranial magnetic stimulation for management of post-stroke impairments: An overview of systematic reviews. J Rehabil Med. 2020;52(2) https://doi.org/10.2340/16501977-2637

46. Nollet H, Van Ham L, Deprez P, Vanderstraeten G. Transcranial magnetic stimulation: review of the technique, basic principles and applications. Vet J. 2003;166(1):28-42. https://doi.org/10.1016/s1090-0233(03)00025-x

47. Chail A, Saini RK, Bhat PS, Srivastava K, Chauhan V. Transcranial magnetic stimulation: A review of its evolution and current applications. Ind Psychiatry J. 2018;27(2):172-80. https://doi.org/10.4103/ipj.ipj_88_18

48. Klomjai W, Katz R, Lackmy-Vallée A. Basic principles of transcranial magnetic stimulation (TMS) and repetitive TMS (rTMS). Ann Phys Rehabil Med. 2015;58(4):208-13. https://doi.org/10.1016/j.rehab.2015.05.005

49. Hallett M. Transcranial magnetic stimulation and the human brain. Nature. 2000;406(6792):147-50. https://doi.org/10.1038/35018000

50. Rossi S, Hallett M, Rossini PM, Pascual-Leone A. Safety, ethical considerations, and application guidelines for the use of transcranial magnetic stimulation in clinical practice and research. Clin Neurophysiol. 2009;120(12):2008-39. https://doi.org/10.1016/j.clinph.2009.08.016

51. Hasey GM. Transcranial magnetic stimulation: using a law of physics to treat psychopathology. J Psychiatry Neurosci. 1999;24(2):97-101. PMID: 10212551

52. Lefaucheur JP. Transcranial magnetic stimulation. Handb Clin Neurol. 2019;160:559-80. https://doi.org/10.1016/b978-0-444-64032-1.00037-0

53. Iglesias AH. Transcranial Magnetic Stimulation as Treatment in Multiple Neurologic Conditions. Curr Neurol Neurosci Rep. 2020;20(1):1. https://doi.org/10.1007/s11910-020-1021-0

54. Burke MJ, Fried PJ, Pascual-Leone A. Transcranial magnetic stimulation: Neurophysiological and clinical applications. Handb Clin Neurol. 2019;163:73-92. https://doi.org/10.1016/b978-0-12-804281-6.00005-7

55. Huang YZ, Edwards MJ, Rounis E, Bhatia KP, Rothwell JC. Theta burst stimulation of the human motor cortex. Neuron. 2005;45(2):201-6. https://doi.org/10.1016/j.neuron.2004.12.033

56. Chervyakov AV, Chernyavsky AY, Sinitsyn DO, Piradov MA. Possible Mechanisms Underlying the Therapeutic Effects of Transcranial Magnetic Stimulation. Front Hum Neurosci. 2015;9:303. https://doi.org/10.3389/fnhum.2015.00303

57. Fujiki M, Steward O. High frequency transcranial magnetic stimulation mimics the effects of ECS in upregulating astroglial gene expression in the murine CNS. Brain Res Mol Brain Res. 1997;44(2):301-8. https://doi.org/10.1016/s0169-328x(96)00232-x

58. Chan P, Eng LF, Lee YL, Lin VW. Effects of pulsed magnetic stimulation of GFAP levels in cultured astrocytes. J Neurosci Res. 1999;55(2):238-44. https://doi.org/10.1002/(sici)1097-4547(19990115)55:2<238::aid-jnr11>3.0.co;2-t

59. Post A, Müller MB, Engelmann M, Keck ME. Repetitive transcranial magnetic stimulation in rats: evidence for a neuroprotective effect in vitro and in vivo. Eur J Neurosci. 1999;11(9):3247-54. https://doi.org/10.1046/j.1460-9568.1999.00747.x

60. Dolgova N, Wei Z, Spink B, Gui L, Hua Q, Truong D, Zhang Z, Zhang Y. Low-Field Magnetic Stimulation Accelerates the Differentiation of Oligodendrocyte Precursor Cells via Non-canonical TGF-β Signaling Pathways. Mol Neurobiol. 2021;58(2):855-66. https://doi.org/10.1007/s12035-020-02157-0

61. Clarke D, Penrose MA, Penstone T, Fuller-Carter PI, Hool LC, Harvey AR, Rodger J, Bates KA. Frequency-specific effects of repetitive magnetic stimulation on primary astrocyte cultures. Restor Neurol Neurosci. 2017;35(6):557-69. https://doi.org/10.3233/rnn-160708

62. Clarke D, Beros J, Bates KA, Harvey AR, Tang AD, Rodger J. Low intensity repetitive magnetic stimulation reduces expression of genes related to inflammation and calcium signalling in cultured mouse cortical astrocytes. Brain Stimul. 2021;14(1):183-91. https://doi.org/10.1016/j.brs.2020.12.007

63. Liu G, Li XM, Tian S, Lu RR, Chen Y, Xie HY, Yu KW, Zhang JJ, Wu JF, Zhu YL, et al. The effect of magnetic stimulation on differentiation of human induced pluripotent stem cells into neuron. J Cell Biochem. 2020;121(10):4130-41. https://doi.org/10.1002/jcb.29647

64. Fregni F, Pascual-Leone A. Transcranial magnetic stimulation for the treatment of depression in neurologic disorders. Curr Psychiatry Rep. 2005;7(5):381-90. https://doi.org/10.1007/s11920-005-0041-4

65. O'Brien AT, Bertolucci F, Torrealba-Acosta G, Huerta R, Fregni F, Thibaut A. Non-invasive brain stimulation for fine motor improvement after stroke: a meta-analysis. Eur J Neurol. 2018;25(8):1017-26. https://doi.org/10.1111/ene.13643

66. Thiel A, Hartmann A, Rubi-Fessen I, Anglade C, Kracht L, Weiduschat N, Kessler J, Rommel T, Heiss WD. Effects of noninvasive brain stimulation on language networks and recovery in early poststroke aphasia. Stroke. 2013;44(8):2240-6. https://doi.org/10.1161/strokeaha.111.000574

67. Nyffeler T, Vanbellingen T, Kaufmann BC, Pflugshaupt T, Bauer D, Frey J, Chechlacz M, Bohlhalter S, Müri RM, Nef T, et al. Theta burst stimulation in neglect after

stroke: functional outcome and response variability origins. Brain. 2019;142(4):992-1008. https://doi.org/10.1093/brain/awz029

68. Zhang C, Zheng X, Lu R, Yun W, Yun H, Zhou X. Repetitive transcranial magnetic stimulation in combination with neuromuscular electrical stimulation for treatment of post-stroke dysphagia. J Int Med Res. 2019;47(2):662-72. https://doi.org/10.1177/0300060518807340

69. Martin DM, McClintock SM, Forster JJ, Lo TY, Loo CK. Cognitive enhancing effects of rTMS administered to the prefrontal cortex in patients with depression: A systematic review and meta-analysis of individual task effects. Depress Anxiety. 2017;34(11):1029-39. https://doi.org/10.1002/da.22658

70. Hallett M. Transcranial magnetic stimulation: a primer. Neuron. 2007;55(2):187-99. https://doi.org/10.1016/j.neuron.2007.06.026

71. Chou YH, Hickey PT, Sundman M, Song AW, Chen NK. Effects of repetitive transcranial magnetic stimulation on motor symptoms in Parkinson disease: a systematic review and meta-analysis. JAMA Neurol. 2015;72(4):432-40. https://doi.org/10.1001/jamaneurol.2014.4380

72. Wagle Shukla A, Shuster JJ, Chung JW, Vaillancourt DE, Patten C, Ostrem J, Okun MS. Repetitive Transcranial Magnetic Stimulation (rTMS) Therapy in Parkinson Disease: A Meta-Analysis. Pm r. 2016;8(4):356-66. https://doi.org/10.1016/j.pmrj.2015.08.009

73. Chung CL, Mak MK, Hallett M. Transcranial Magnetic Stimulation Promotes Gait Training in Parkinson Disease. Ann Neurol. 2020;88(5):933-45. https://doi.org/10.1002/ana.25881

74. Gao C, Liu J, Tan Y, Chen S. Freezing of gait in Parkinson's disease: pathophysiology, risk factors and treatments. Transl Neurodegener. 2020;9:12. https://doi.org/10.1186/s40035-020-00191-5

75. Nardone R, Tezzon F, Höller Y, Golaszewski S, Trinka E, Brigo F. Transcranial magnetic stimulation (TMS)/repetitive TMS in mild cognitive impairment and Alzheimer's disease. Acta Neurol Scand. 2014;129(6):351-66. https://doi.org/10.1111/ane.12223

76. Chou YH, Ton That V, Sundman M. A systematic review and meta-analysis of rTMS effects on cognitive enhancement in mild cognitive impairment and Alzheimer's disease. Neurobiol Aging. 2020;86:1-10. https://doi.org/10.1016/j.neurobiolaging.2019.08.020

77. Liu M, Fan S, Xu Y, Cui L. Non-invasive brain stimulation for fatigue in multiple sclerosis patients: A systematic review and meta-analysis. Mult Scler Relat Disord. 2019;36:101375. https://doi.org/10.1016/j.msard.2019.08.017

78. Lin Y, Jin J, Lv R, Luo Y, Dai W, Li W, Tang Y, Wang Y, Ye X, Lin WJ. Repetitive transcranial magnetic stimulation increases the brain's drainage efficiency in a mouse model of Alzheimer's disease. Acta Neuropathol Commun. 2021;9(1):102. https://doi.org/10.1186/s40478-021-01198-3

79. Shiiba S, Yamamoto S, Sasaki H, Nishi M, Ishikawa K, Yasuda S, Tokuda N, Nakanishi O, Ishikawa T. Cutaneous Magnetic Stimulation Reduces Rat Chronic Pain via

Activation of the Supra-Spinal Descending Pathway. Cell Mol Neurobiol. 2012;32(2):245-53. https://doi.org/10.1007/s10571-011-9756-4

80. Yang L, Wang SH, Hu Y, Sui YF, Peng T, Guo TC. Effects of Repetitive Transcranial Magnetic Stimulation on Astrocytes Proliferation and nNOS Expression in Neuropathic Pain Rats. Curr Med Sci. 2018;38(3):482-90. https://doi.org/10.1007/s11596-018-1904-3

81. Cui M, Ge H, Zeng H, Yan H, Zhang L, Feng H, Chen Y. Repetitive Transcranial Magnetic Stimulation Promotes Neural Stem Cell Proliferation and Differentiation after Intracerebral Hemorrhage in Mice. Cell Transplant. 2019;28(5):568-84. https://doi.org/10.1177/0963689719834870

82. Hong Y, Liu Q, Peng M, Bai M, Li J, Sun R, Guo H, Xu P, Xie Y, Li Y, et al. High-frequency repetitive transcranial magnetic stimulation improves functional recovery by inhibiting neurotoxic polarization of astrocytes in ischemic rats. J Neuroinflammation. 2020;17(1):150. https://doi.org/10.1186/s12974-020-01747-y

83. Medina-Fernandez FJ, Luque E, Aguilar-Luque M, Aguera E, Feijoo M, Garcia-Maceira FI, Escribano BM, Pascual-Leone A, Drucker-Colin R, Tunez I. Transcranial magnetic stimulation modifies astrocytosis, cell density and lipopolysaccharide levels in experimental, autoimmune encephalomyelitis. Life Sci. 2017;169:20-6. https://doi.org/10.1016/j.lfs.2016.11.011

84. Chalfouh C, Guillou C, Hardouin J, Delarue Q, Li X, Duclos C, Schapman D, Marie JP, Cosette P, Guérout N. The Regenerative Effect of Trans-spinal Magnetic Stimulation After Spinal Cord Injury: Mechanisms and Pathways Underlying the Effect. Neurotherapeutics. 2020;17(4):2069-88. https://doi.org/10.1007/s13311-020-00915-5

85. Feng S, Wang S, Sun S, Su H, Zhang L. Effects of combination treatment with transcranial magnetic stimulation and bone marrow mesenchymal stem cell transplantation or Raf inhibition on spinal cord injury in rats. Mol Med Rep. 2021;23(4) https://doi.org/10.3892/mmr.2021.11934

86. Kim JY, Choi GS, Cho YW, Cho H, Hwang SJ, Ahn SH. Attenuation of spinal cord injury-induced astroglial and microglial activation by repetitive transcranial magnetic stimulation in rats. J Korean Med Sci. 2013;28(2):295-9. https://doi.org/10.3346/jkms.2013.28.2.295

87. Sekar S, Zhang Y, Miranzadeh Mahabadi H, Parvizi A, Taghibiglou C. Low-Field Magnetic Stimulation Restores Cognitive and Motor Functions in the Mouse Model of Repeated Traumatic Brain Injury: Role of Cellular Prion Protein. J Neurotrauma. 2019;36(22):3103-14. https://doi.org/10.1089/neu.2018.5918

88. Li K, Wang X, Jiang Y, Zhang X, Liu Z, Yin T, Yang Z. Early intervention attenuates synaptic plasticity impairment and neuroinflammation in 5xFAD mice. J Psychiatr Res. 2021;136:204-16. https://doi.org/10.1016/j.jpsychires.2021.02.007

89. Caglayan AB, Beker MC, Caglayan B, Yalcin E, Caglayan A, Yulug B, Hanoglu L, Kutlu S, Doeppner TR, Hermann DM, et al. Acute and Post-acute Neuromodulation Induces Stroke Recovery by Promoting Survival Signaling, Neurogenesis, and Pyramidal Tract Plasticity. Front Cell Neurosci. 2019;13:144. https://doi.org/10.3389/fncel.2019.00144

90. Yang L, Su Y, Guo F, Zhang H, Zhao Y, Huang Q, Xu H. Deep rTMS Mitigates Behavioral and Neuropathologic Anomalies in Cuprizone-Exposed Mice Through

Reducing Microglial Proinflammatory Cytokines. Front Integr Neurosci. 2020;14:556839. https://doi.org/10.3389/fnint.2020.556839

91. Delarue Q, Robac A, Massardier R, Marie JP, Guerout N. Comparison of the effects of two therapeutic strategies based on olfactory ensheathing cell transplantation and repetitive magnetic stimulation after spinal cord injury in female mice. Journal of Neuroscience Research. 2021;99(7):1835-49. https://doi.org/10.1002/jnr.24836

92. Wang Z, Baharani A, Wei Z, Truong D, Bi X, Wang F, Li XM, Verge VMK, Zhang Y. Low field magnetic stimulation promotes myelin repair and cognitive recovery in chronic cuprizone mouse model. Clin Exp Pharmacol Physiol. 2021;48(8):1090-102. https://doi.org/10.1111/1440-1681.13490

93. Huerta PT, Volpe BT. Transcranial magnetic stimulation, synaptic plasticity and network oscillations. J Neuroeng Rehabil. 2009;6:7. https://doi.org/10.1186/1743-0003-6-7

94. Chieffo R, Ferrari F, Battista P, Houdayer E, Nuara A, Alemanno F, Abutalebi J, Zangen A, Comi G, Cappa SF, et al. Excitatory deep transcranial magnetic stimulation with H-coil over the right homologous Broca's region improves naming in chronic post-stroke aphasia. Neurorehabil Neural Repair. 2014;28(3):291-8. https://doi.org/10.1177/1545968313508471

95. Chieffo R, De Prezzo S, Houdayer E, Nuara A, Di Maggio G, Coppi E, Ferrari L, Straffi L, Spagnolo F, Velikova S, et al. Deep repetitive transcranial magnetic stimulation with H-coil on lower limb motor function in chronic stroke: a pilot study. Arch Phys Med Rehabil. 2014;95(6):1141-7. https://doi.org/10.1016/j.apmr.2014.02.019

96. Wang Q, Zhang D, Zhao YY, Hai H, Ma YW. Effects of high-frequency repetitive transcranial magnetic stimulation over the contralesional motor cortex on motor recovery in severe hemiplegic stroke: A randomized clinical trial. Brain Stimul. 2020;13(4):979-86. https://doi.org/10.1016/j.brs.2020.03.020

97. Sasaki N, Mizutani S, Kakuda W, Abo M. Comparison of the effects of high- and low-frequency repetitive transcranial magnetic stimulation on upper limb hemiparesis in the early phase of stroke. J Stroke Cerebrovasc Dis. 2013;22(4):413-8. https://doi.org/10.1016/j.jstrokecerebrovasdis.2011.10.004

98. Luo J, Zheng H, Zhang L, Zhang Q, Li L, Pei Z, Hu X. High-Frequency Repetitive Transcranial Magnetic Stimulation (rTMS) Improves Functional Recovery by Enhancing Neurogenesis and Activating BDNF/TrkB Signaling in Ischemic Rats. Int J Mol Sci. 2017;18(2) https://doi.org/10.3390/ijms18020455

99. Roque C, Pinto N, Patto MV, Baltazar G. Astrocytes contribute to the neuronal recovery promoted by high-frequency repetitive magnetic stimulation in in vitro models of ischemia. Journal of Neuroscience Research. 2021;99(5):1414-32. https://doi.org/10.1002/jnr.24792

100. Roque C, Baltazar G. Impact of Astrocytes on the Injury Induced by In Vitro Ischemia. Cell Mol Neurobiol. 2017;37(8):1521-8. https://doi.org/10.1007/s10571-017-0483-3

101. Haugeto O, Ullensvang K, Levy LM, Chaudhry FA, Honoré T, Nielsen M, Lehre KP, Danbolt NC. Brain glutamate transporter proteins form homomultimers. J Biol Chem. 1996;271(44):27715-22. https://doi.org/10.1074/jbc.271.44.27715

102. Stone WL, Leavitt L, Varacallo M. Physiology, Growth Factor. StatPearls StatPearls Publishing; 2022. pp.

103. Gao F, Wang S, Guo Y, Wang J, Lou M, Wu J, Ding M, Tian M, Zhang H. Protective effects of repetitive transcranial magnetic stimulation in a rat model of transient cerebral ischaemia: a microPET study. Eur J Nucl Med Mol Imaging. 2010;37(5):954-61. https://doi.org/10.1007/s00259-009-1342-3

104. Sasso V, Bisicchia E, Latini L, Ghiglieri V, Cacace F, Carola V, Molinari M, Viscomi MT. Repetitive transcranial magnetic stimulation reduces remote apoptotic cell death and inflammation after focal brain injury. J Neuroinflammation. 2016;13(1):150. https://doi.org/10.1186/s12974-016-0616-5

105. Cacace F, Mineo D, Viscomi MT, Latagliata EC, Mancini M, Sasso V, Vannelli A, Pascucci T, Pendolino V, Marcello E, et al. Intermittent theta-burst stimulation rescues dopamine-dependent corticostriatal synaptic plasticity and motor behavior in experimental parkinsonism: Possible role of glial activity. Mov Disord. 2017;32(7):1035-46. https://doi.org/10.1002/mds.26982

106. Vucic S, Pavey N, Haidar M, Turner BJ, Kiernan MC. Cortical hyperexcitability: Diagnostic and pathogenic biomarker of ALS. Neurosci Lett. 2021;759:136039. https://doi.org/10.1016/j.neulet.2021.136039

107. Junior GG (2020) Effects of High Frequency repetitive Magnetic Stimulation on astrocytes in an ischemic cell model.Universidade da Beira Interior.

108. Chamorro Á, Dirnagl U, Urra X, Planas AM. Neuroprotection in acute stroke: targeting excitotoxicity, oxidative and nitrosative stress, and inflammation. Lancet Neurol. 2016;15(8):869-81. https://doi.org/10.1016/s1474-4422(16)00114-9

109. Becerra-Calixto A, Cardona-Gómez GP. The Role of Astrocytes in Neuroprotection after Brain Stroke: Potential in Cell Therapy. Front Mol Neurosci. 2017;10:88. https://doi.org/10.3389/fnmol.2017.00088

110. Liu Z, Chopp M. Astrocytes, therapeutic targets for neuroprotection and neurorestoration in ischemic stroke. Prog Neurobiol. 2016;144:103-20. https://doi.org/10.1016/j.pneurobio.2015.09.008

111. Pajarillo E, Rizor A, Lee J, Aschner M, Lee E. The role of astrocytic glutamate transporters GLT-1 and GLAST in neurological disorders: Potential targets for neurotherapeutics. Neuropharmacology. 2019;161:107559. https://doi.org/10.1016/j.neuropharm.2019.03.002

112. Delyfer MN, Simonutti M, Neveux N, Léveillard T, Sahel JA. Does GDNF exert its neuroprotective effects on photoreceptors in the rd1 retina through the glial glutamate transporter GLAST? Mol Vis. 2005;11:677-87. PMID: 16163265

113. Rao VL, Dogan A, Todd KG, Bowen KK, Kim BT, Rothstein JD, Dempsey RJ. Antisense knockdown of the glial glutamate transporter GLT-1, but not the neuronal glutamate transporter EAAC1, exacerbates transient focal cerebral ischemia-induced neuronal damage in rat brain. J Neurosci. 2001;21(6):1876-83. https://doi.org/10.1523/jneurosci.21-06-01876.2001

114. Weller ML, Stone IM, Goss A, Rau T, Rova C, Poulsen DJ. Selective overexpression of excitatory amino acid transporter 2 (EAAT2) in astrocytes enhances

neuroprotection from moderate but not severe hypoxia-ischemia. Neuroscience. 2008;155(4):1204-11. https://doi.org/10.1016/j.neuroscience.2008.05.059

115. Ikeda T, Kobayashi S, Morimoto C. Effects of repetitive transcranial magnetic stimulation on ER stress-related genes and glutamate, γ-aminobutyric acid and glycine transporter genes in mouse brain. Biochem Biophys Rep. 2019;17:10-6. https://doi.org/10.1016/j.bbrep.2018.10.015

116. Mancic B, Stevanovic I, Ilic TV, Djuric A, Stojanovic I, Milanovic S, Ninkovic M. Transcranial theta-burst stimulation alters GLT-1 and vGluT1 expression in rat cerebellar cortex. Neurochem Int. 2016;100:120-7. https://doi.org/10.1016/j.neuint.2016.09.009

117. Kilic U, Kilic E, Dietz GP, Bähr M. Intravenous TAT-GDNF is protective after focal cerebral ischemia in mice. Stroke. 2003;34(5):1304-10. https://doi.org/10.1161/01.str.0000066869.45310.50

118. Lee E, Sidoryk-Wegrzynowicz M, Yin Z, Webb A, Son DS, Aschner M. Transforming growth factor-α mediates estrogen-induced upregulation of glutamate transporter GLT-1 in rat primary astrocytes. Glia. 2012;60(7):1024-36. https://doi.org/10.1002/glia.22329

119. Naskar R, Vorwerk CK, Dreyer EB. Concurrent downregulation of a glutamate transporter and receptor in glaucoma. Invest Ophthalmol Vis Sci. 2000;41(7):1940-4. PMID: 10845620

120. Bonde C, Sarup A, Schousboe A, Gegelashvili G, Noraberg J, Zimmer J. GDNF pre-treatment aggravates neuronal cell loss in oxygen-glucose deprived hippocampal slice cultures: a possible effect of glutamate transporter up-regulation. Neurochem Int. 2003;43(4-5):381-8. https://doi.org/10.1016/s0197-0186(03)00025-1

121. Nicole O, Ali C, Docagne F, Plawinski L, MacKenzie ET, Vivien D, Buisson A. Neuroprotection mediated by glial cell line-derived neurotrophic factor: involvement of a reduction of NMDA-induced calcium influx by the mitogen-activated protein kinase pathway. J Neurosci. 2001;21(9):3024-33. https://doi.org/10.1523/jneurosci.21-09-03024.2001

122. Iwata-Ichikawa E, Kondo Y, Miyazaki I, Asanuma M, Ogawa N. Glial cells protect neurons against oxidative stress via transcriptional up-regulation of the glutathione synthesis. J Neurochem. 1999;72(6):2334-44. https://doi.org/10.1046/j.1471-4159.1999.0722334.x

123. Beker M, Caglayan AB, Beker MC, Altunay S, Karacay R, Dalay A, Altintas MO, Kose GT, Hermann DM, Kilic E. Lentivirally administered glial cell line-derived neurotrophic factor promotes post-ischemic neurological recovery, brain remodeling and contralesional pyramidal tract plasticity by regulating axonal growth inhibitors and guidance proteins. Exp Neurol. 2020;331:113364. https://doi.org/10.1016/j.expneurol.2020.113364

124. Lee JY, Kim HS, Kim SH, Kim HS, Cho BP. Combination of Human Mesenchymal Stem Cells and Repetitive Transcranial Magnetic Stimulation Enhances Neurological Recovery of 6-Hydroxydopamine Model of Parkinsonian's Disease. Tissue Eng Regen Med. 2020;17(1):67-80. https://doi.org/10.1007/s13770-019-00233-8

125. Lee JY, Kim SH, Ko AR, Lee JS, Yu JH, Seo JH, Cho BP, Cho SR. Therapeutic effects of repetitive transcranial magnetic stimulation in an animal model of Parkinson's disease. Brain Res. 2013;1537:290-302. https://doi.org/10.1016/j.brainres.2013.08.051

126. Lee JY, Park HJ, Kim JH, Cho BP, Cho SR, Kim SH. Effects of low- and high-frequency repetitive magnetic stimulation on neuronal cell proliferation and growth factor expression: A preliminary report. Neurosci Lett. 2015;604:167-72. https://doi.org/10.1016/j.neulet.2015.07.038

127. Wang HY, Crupi D, Liu J, Stucky A, Cruciata G, Di Rocco A, Friedman E, Quartarone A, Ghilardi MF. Repetitive transcranial magnetic stimulation enhances BDNF-TrkB signaling in both brain and lymphocyte. J Neurosci. 2011;31(30):11044-54. https://doi.org/10.1523/jneurosci.2125-11.2011

128. Vlachos A, Müller-Dahlhaus F, Rosskopp J, Lenz M, Ziemann U, Deller T. Repetitive magnetic stimulation induces functional and structural plasticity of excitatory postsynapses in mouse organotypic hippocampal slice cultures. J Neurosci. 2012;32(48):17514-23. https://doi.org/10.1523/jneurosci.0409-12.2012

Chapter 8

Supplementary material

Table 1 Composition of the solutions used.

Solution	Reagent	pH	Concentration	Reference
Hank's Balanced Salt Solution (HBSS)	$CaCl_2$	7.2	1.26 mM	Panreac, C001
	KCl		5.36 mM	PanReac AppliChem, A2939
	KH_2PO_4		0.44 mM	Chem-lab, 15004CL0014612
	$MgCl_2$		0.49 mM	LabChem, MGCH-06P-1K0
	NaCl		139.9 mM	Fisher Scientific, S271-500
	$NaHCO_3$		4.17 mM	Sigma-Aldrich, S5761
	Na_2HPO_4		3.38 mM	Fisher Bioreagents, BP332-500
	45% anhydrous D-glucose		5.56 mM	Fisher Scientific, G/0450/60
Loading Buffer (6x)	Tris	-	100 mM	Fisher Scientific, M-27435
	Glycine		100 mM	Fisher Scientific, BP381-1
	SDS		139 mM	Panreac, 142363.1211
	Urea		8 M	Acros, 140750010
	Bromophenol blue		1.46 x 10^{-4} mM	Amresco, 0449
	β-mercaptoethanol		1.42 M	Merck, 8.05740.1000
Lysis buffer	Tris	7.5	25 mM	Fisher Scientific, M-27435
	EDTA		2.5 mM	Panreac, 131669.1211
	EGTA		2.5 mM	Sigma-Aldrich, E4378
	Triton X100		0.2%	Fisher Scientific, BP151-500
	Na_3VO_4		2 mM	Sigma-Aldrich, S6508-10G
	complete EDTA free protease inhibitor cocktail tablets		4%	Roche, 04693132001
M10cG medium	MEM	7.2	9.6 g/L	Sigma-Aldrich, M0268
	$NaHCO_3$		0.026 M	Sigma-Aldrich, S5761
	Glutamine		0.49 mM	Sigma-Aldrich, G3126
	Insulin from bovine pancreas		5 mg/L	Sigma-Aldrich, I5500
	45% anhydrous D-glucose		3.375 g/L	Fisher Scientific, G/0450/60
	Penicillin/ Streptomycin		12 U/ml	Biochrom, A2213
	heat-not Inactivated FBS		10%	Biochrom AG, BCS0615

Neurobasal medium	Neurobasal Medium	7.2	Gibco, 21103-049	
	B27		2%	Gibco, 17504044
	Glutamate		25 µM	Sigma-Aldrich, G8415
	Glutamine		0.5 mM	Sigma-Aldrich, G3126
	Gentamicine		120 µg/mL	Sigma-Aldrich, G1272
	FBS		10%	Biochrom AG, BCS0615
poly-D-Lysine (PDL)	H_3BO_3	8.4	0.15 M	Chem-Lab, CL00.0216.1000
	PDL		0.1 mg/ml	Sigma-Aldrich, P1149
PBS	NaCl	7.2	140 mM	Fisher Scientific, S271-500
	KCl		2.7 mM	PanReac AppliChem, A2939
	KH_2PO_4		1.5 mM	Honeywell, 60216
	Na_2HPO_4		8.1 mM	Fisher Bioreagents, BP332-500
Resolving Gel	Acrylamide 30%		1.64 M	Panreac, A3626,0500
	Tris 1.5 M, pH 8.8		373 mM	Fisher Scientific, M-27435
	SDS		3.45 mM	Panreac, 142363.1211
	PSA		11.35 mM	Panreac, 131138.1610
	TEMED		3.29 mM	Acros, 138455000
Running Buffer	Tris	-	25 mM	Fisher Scientific, M-27435
	Glycine		192 mM	Fisher Scientific, BP381-1
	SDS		3.45 mM	Panreac, 142363.1211
Stacking Gel	Acrylamide 30%		531 mM	Panreac, A3626,0500
	Tris 0.5 M, pH 6.8		124 mM	Fisher Scientific, M-27435
	SDS		3.45 mM	Panreac, 142363.1211
	PSA		11.35 mM	Panreac, 131138.1610
	TEMED		6.58 mM	Acros, 138455000
Transfer Buffer	Tris	-	25 mM	Fisher Scientific, M-27435
	Glycine		192 mM	Fisher Scientific, BP381-1
	SDS		0.173 mM	Panreac, 142363.1211
	Methanol		10%	Fisher Chemical, M/4000/17
Tris Buffered Saline with 0.1% Tween (TBS-T)	Tris	-	20 mM	Fisher Scientific, M-27435
	NaCl		140 mM	Fisher Scientific, S271-500
	Tween 20		2.1×10^{-3} mM	Fisher Scientific, BP337-500

Table 2 Statistical analysis.

	F (DFn, DFd)	P value	post-hoc test for multiple comparison correction		P value
Figure 6.b	F (3, 55) = 2.264	0.0911	Bonferroni's multiple comparisons test	Control vs. HF-rMS	0.7434
				Control vs. OGD	0.3044
				Control vs. OGD+HF-rMS	0.0738
				HF-rMS vs. OGD	0.8702
				HF-rMS vs. OGD+HF-rMS	0.4611
				OGD vs. OGD+HF-rMS	0.9034

	F (DFn, DFd)	P value	post-hoc test for multiple comparison correction		P value
Figure 6.c	F (3, 55) = 4.328	0.0083	Bonferroni's multiple comparisons test	Control vs. HF-rMS	0.7861
				Control vs. OGD	0.1479
				Control vs. OGD+HF-rMS	0.0072
				HF-rMS vs. OGD	0.6048
				HF-rMS vs. OGD+HF-rMS	0.081
				OGD vs. OGD+HF-rMS	0.6541

	F (DFn, DFd)	P value	post-hoc test for multiple comparison correction		P value
Figure 7.b	F (3, 55) = 1.653	0.1878	Bonferroni's multiple comparisons test	Control vs. HF-rMS	0.9992
				Control vs. OGD	0.6013
				Control vs. OGD+HF-rMS	0.2441
				HF-rMS vs. OGD	0.6808
				HF-rMS vs. OGD+HF-rMS	0.3036
				OGD vs. OGD+HF-rMS	0.9278

	F (DFn, DFd)	P value	post-hoc test for multiple comparison correction		P value
Figure 9.b	F (3, 24) = 4.114	0.0173	Bonferroni's multiple comparisons test	Control vs. HF-rMS	>0.9999
				Control vs. OGD	>0.9999
				Control vs. OGD+HF-rMS	0.0277
				HF-rMS vs. OGD	>0.9999
				HF-rMS vs. OGD+HF-rMS	0.0478
				OGD vs. OGD+HF-rMS	0.1512

	F (DFn, DFd)	P value	post-hoc test for multiple comparison correction		P value
Figure 9.c	F (3, 12) = 5.079	0.0169	Bonferroni's multiple comparisons test	Control vs. HF-rMS	>0.9999
				Control vs. OGD	0.4947
				Control vs. OGD+HF-rMS	0.031
				HF-rMS vs. OGD	0.7286

				HF-rMS vs. OGD+HF-rMS	0.0473
				OGD vs. OGD+HF-rMS	0.9332

	F (DFn, DFd)	P value	post-hoc test for multiple comparison correction		P value
Figure 10	F (9, 18) = 13.62	<0.0001	Bonferroni's multiple comparisons test	non-CM vs. non-CM OGD	0.0006
				non-CM vs. astrocyte-CM	>0.9999
				non-CM vs. astrocyte-CM OGD	<0.0001
				non-CM vs. astrocyte-CM+HF-rMS	>0.9999
				non-CM vs. astrocyte-CM+HF-rMS OGD	<0.0001
				astrocyte-CM vs. astrocyte-CM - GDNF	0.2125
				astrocyte-CM OGD vs. astrocyte-CM OGD - GDNF	>0.9999
				astrocyte-CM+HF-rMS vs. astrocyte-CM+HF-rMS - GDNF	0.3746
				astrocyte-CM+HF-rMS OGD vs. astrocyte-CM+HF-rMS OGD - GDNF	>0.9999
				astrocyte-CM OGD vs. astrocyte-CM+HF-rMS OGD	>0.9999

	F (DFn, DFd)	P value	post-hoc test for multiple comparison correction		P value
Figure 11.a	F (9, 50) = 19.09	<0.0001	Bonferroni's multiple comparisons test	non-CM vs. non-CM OGD	0.003
				non-CM vs. astrocyte-CM	0.8924
				non-CM vs. astrocyte-CM OGD	0.1627
				non-CM vs. astrocyte-CM+HF-rMS	0.0312
				non-CM vs. astrocyte-CM+HF-rMS OGD	0.0642
				astrocyte-CM vs. astrocyte-CM - GDNF	<0.0001
				astrocyte-CM OGD vs. astrocyte-CM OGD - GDNF	0.4686
				astrocyte-CM+HF-rMS vs. astrocyte-CM+HF-rMS - GDNF	<0.0001
				astrocyte-CM+HF-rMS OGD vs. astrocyte-CM+HF-rMS OGD - GDNF	<0.0001
				astrocyte-CM OGD vs. astrocyte-CM+HF-rMS OGD	<0.0001

	F (DFn, DFd)	P value	post-hoc test for multiple comparison correction		P value
Figure 11.b	F (9, 50) = 18.22	<0.0001	Bonferroni's multiple comparisons test	non-CM vs. non-CM OGD	0.0041
				non-CM vs. astrocyte-CM	>0.9999
				non-CM vs. astrocyte-CM OGD	0.0474
				non-CM vs. astrocyte-CM+HF-rMS	0.0002
				non-CM vs. astrocyte-CM+HF-rMS OGD	0.1641
				astrocyte-CM vs. astrocyte-CM - GDNF	0.0008
				astrocyte-CM OGD vs. astrocyte-CM OGD - GDNF	>0.9999
				astrocyte-CM+HF-rMS vs. astrocyte-CM+HF-rMS - GDNF	<0.0001

				astrocyte-CM+HF-rMS OGD vs. astrocyte-CM+HF-rMS OGD - GDNF	<0.0001
				astrocyte-CM OGD vs. astrocyte-CM+HF-rMS OGD	<0.0001

	F (DFn, DFd)	P value	post-hoc test for multiple comparison correction		P value
Figure 11.c	F (9, 20) = 120.7	<0.0001	Bonferroni's multiple comparisons test	non-CM vs. non-CM OGD	<0.0001
				non-CM vs. astrocyte-CM	0.0035
				non-CM vs. astrocyte-CM OGD	<0.0001
				non-CM vs. astrocyte-CM+HF-rMS	<0.0001
				non-CM vs. astrocyte-CM+HF-rMS OGD	<0.0001
				astrocyte-CM vs. astrocyte-CM - GDNF	<0.0001
				astrocyte-CM OGD vs. astrocyte-CM OGD - GDNF	0.1919
				astrocyte-CM+HF-rMS vs. astrocyte-CM+HF-rMS - GDNF	<0.0001
				astrocyte-CM+HF-rMS OGD vs. astrocyte-CM+HF-rMS OGD - GDNF	<0.0001
				astrocyte-CM OGD vs. astrocyte-CM+HF-rMS OGD	<0.0001

	F (DFn, DFd)	P value	post-hoc test for multiple comparison correction		P value
Figure 12	F (9, 18) = 38.79	<0.0001	Bonferroni's multiple comparisons test	non-CM vs. non-CM OGD	0.0057
				non-CM vs. astrocyte-CM	0.1258
				non-CM vs. astrocyte-CM OGD	>0.9999
				non-CM vs. astrocyte-CM+HF-rMS	<0.0001
				non-CM vs. astrocyte-CM+HF-rMS OGD	<0.0001
				astrocyte-CM vs. astrocyte-CM - GDNF	0.0019
				astrocyte-CM OGD vs. astrocyte-CM OGD - GDNF	0.2768
				astrocyte-CM+HF-rMS vs. astrocyte-CM+HF-rMS - GDNF	<0.0001
				astrocyte-CM+HF-rMS OGD vs. astrocyte-CM+HF-rMS OGD - GDNF	<0.0001
				astrocyte-CM OGD vs. astrocyte-CM+HF-rMS OGD	<0.0001

Chapter 9

Attachments

Poster presented at VI Symposium of the Portuguese Glia Network named "Neurons Injured by Ischemia can be Rescued Through the Modulation of Astrocytes by HF-rMS"

Neurons Injured by Ischemia can be Rescued Through the Modulation of Astrocytes by HF-rMS

Susana A. Ferreira[1,(*)], Nuno Pinto[1,2], Maria Vaz Patto[1,2], Graça Baltazar[1,2]

[1] Centro de Investigação em Ciências da Saúde (CICS-UBI), and [2] Faculdade de Ciências da Saúde, Universidade da Beira Interior, Av. Infante D. Henrique, 6200-506 Covilhã, Portugal.
[(*)] *Email:* susana.alves.ferreira@fcsaude.ubi.pt

Introduction

Ischemic stroke is caused by the reduction or blockage of blood flow to the brain [1] and is the third most common cause of death in Portugal [2]. High-frequency repetitive magnetic stimulation (HF-rMS) has shown potential in promoting the recovery of ischemic stroke patients [3-7]. However, data regarding HF-rMS cellular effects are scarce and are mainly focused on neurons. Our group showed that the secretome of astrocytes subjected to rMS promotes neuronal recovery, but the mediators responsible for the neuroprotective effect have not yet been identified. **Thus, this study aims to identify the mechanisms triggered HF-rMS that contribute to the neuroprotective action of astrocytes.**

Experimental Design

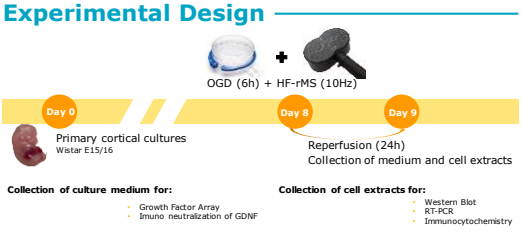

Results

1. HF-rMS increases the expression of EAAT1 glutamate transporter

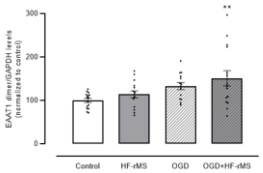

Figure 1. Effect of HF-rMS on glutamate transporter levels. The error bars represent the mean ± SEM of six independent experiments performed in duplicate or triplicate, each sample is represented by a dot. (**P<0.01 to control).

2. HF-rMS promotes the expression and release of GDNF by astrocytes

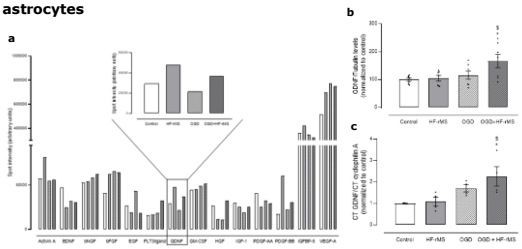

Figure 2. a. Semi-quantitative detection of GDNF levels in astrocyte culture medium through an antibody array (RayBio® C-Series Rat Growth Factor Array 1). **b.** GDNF protein levels determined by western blot. **c.** Gdnf mRNA expression levels determined by RT-PCR in astrocyte-enriched cultures. (*P<0.05 to control, $P<0.05 to HF-rMS)

3. Depletion of GDNF from the CM of HF-rMS-stimulated astrocytes hampers the protection exerted by this CM on ischemia-induced neurite degeneration

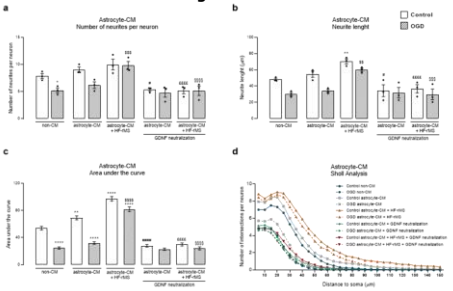

Figure 3. GDNF neutralization hampers the effects of astrocyte-CM on ischemia-induced neurite degeneration. **a.** Number of neurites per neuron. **b.** Neurite length. **c.** Area under the curve from Sholl analysis. **d.** Number of intersections per neuron on the distance to soma determined by Sholl analysis. *P<0.05, **P<0.01, ***P<0.0001 compared to non-CM; #P<0.05, ####P<0.0001 compared to Control; £££££P<0.0001 compared to HF-rMS; $$P<0.01, $$$P<0.001, $$$$P<0.0001 compared to OGD, and §§§§P<0.001, §§§§P<0.0001 compared to OGD + HF-rMS.

4. Neutralization of GDNF present in CM from HF-rMS-stimulated astrocytes impedes the effect of this CM on ischemia-induced reduction of c-Fos expressing neurons

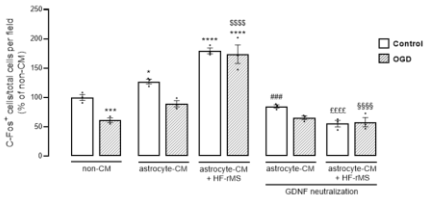

Figure 4. Neutralization of GDNF in CM from HF-rMS-stimulated astrocytes reduces the number of neurons expressing c-Fos. *P<0.05, ***P<0.001, ****P<0.0001 compared to non-CM; ###P<0.001 compared to Control; £££££P<0.0001 compared to HF-rMS; $$$$P<0.0001 compared to OGD, and §§§§P<0.0001 compared to OGD + HF-rMS.

Conclusions

- HF-rMS increases the levels of glutamate transporter EAAT1 in cortical cultures exposed to OGD, suggesting that HF-rMS may decrease the excitotoxicity associated with the ischemic injury.
- GDNF released by HF-rMS-exposed astrocytes contributes to the neuroprotection promoted by HF-rMS in a model of ischemic injury.

References

[1] Radak, D., *et al.* Curr Vasc Pharmacol 2017. **15**(2): p. 115-122.
[2] Freitas-Silva, M., *et al.* Clin Neurol Neurosurg 2021. **203**: p. 106564.
[3] Sasaki, N., et al. J Stroke CerebrovascDis, 2013. **22**(4): p. 413-8.
[4] Dionísio, A., et al. J Stroke CerebrovascDis, 2018. **27**(1): p. 1-31.
[5] Chieffo, R., et al. NeurorehabilNeuralRepair, 2014. **28**(3): p. 291-8.
[6] Chieffo, R., et al. Arch Phys Med Rehabil, 2014. **95**(6): p. 1141-7.
[7] Wang, Q., et al. Brain Stimul, 2020. **13**(4): p. 979-986.

FCT COMPETE 2020 PORTUGAL 2020

Certificate of Poster presented at VI Symposium of the Portuguese Glia Network

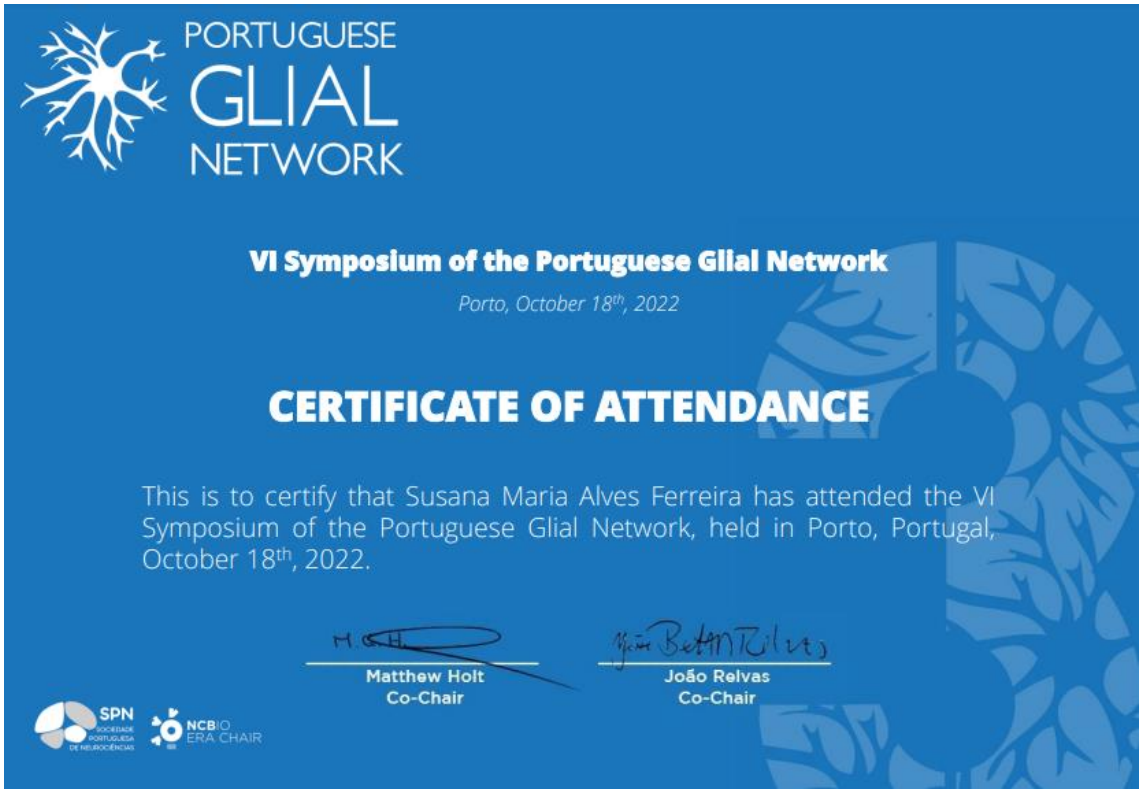

Poster presented at XVII International CICS-UBI Symposium named “Contribution of astrocytes to the neuroprotective effect mediated by rMS”

CICS-UBI
Centro de Investigação em Ciências da Saúde
Health Sciences Research Centre

FACULDADE CIÊNCIAS DA SAÚDE

Contribution of astrocytes to the neuroprotective effect mediated by rMS

Susana A. Ferreira[1,(*)], Nuno Pinto[1,2], Maria Vaz Patto[1,2], Graça Baltazar [1,2]

[1] Centro de Investigação em Ciências da Saúde (CICS-UBI), and [2] Faculdade de Ciências da Saúde, Universidade da Beira Interior, Av. Infante D. Henrique, 6200-506 Covilhã, Portugal.
(*) *Email:* susana.alves.ferreira@fcsaude.ubi.pt

Introduction

Ischemic stroke is caused by the reduction or blockage of blood flow to the brain [1] and is the third most common cause of death in Portugal [2]. High-frequency repetitive magnetic stimulation (HF-rMS) has shown potential in promoting the recovery of ischemic stroke patients [3-7]. However, data regarding HF-rMS cellular effects are scarce and are mainly focused on neurons. Our group showed that the secretome of astrocytes subjected to rMS promotes neuronal recovery, but the mediators responsible for the neuroprotective effect have not yet been identified.

Thus, this study aims to determine the effects triggered by astrocytes that contribute to their neuroprotective action and to identify the trophic factors released by astrocytes in response to HF-rMS.

Experimental Design

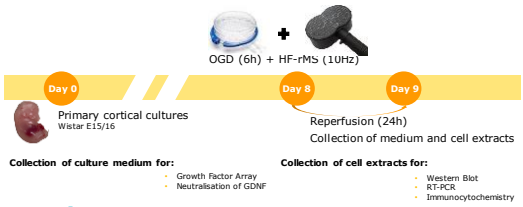

Results

1. HF-rMS increases the expression of EAAT1 glutamate transporter

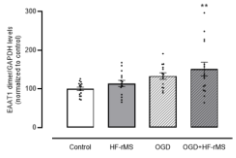

Figure 1. Effect of HF-rMS on glutamate transporter levels. The error bars represent the mean ± SEM of six independent experiments performed in duplicate or triplicate, each sample is represented by a dot. (** P < 0.01 to control).

2. HF-rMS promotes the expression and release of GDNF by astrocytes

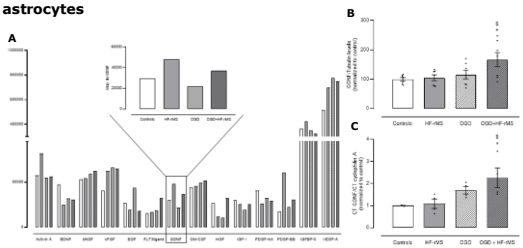

Figure 2. A. Semi-quantitative detection of GDNF levels in astrocyte culture medium through an antibody array (RayBio® C-Series Rat Growth Factor Array 1). **B.** GDNF protein levels determined by western blot. **C.** Gdnf mRNA expression levels determined by RT-PCR in astrocyte-enriched cultures. (** P < 0.01 to control, $ P < 0.05 to HF-rMS, # P < 0.05 to OGD).

3. Depletion of GDNF from the CM of HF-rMS-stimulated astrocytes hampers the protection exerted by this CM on ischemia-induced neurite degeneration

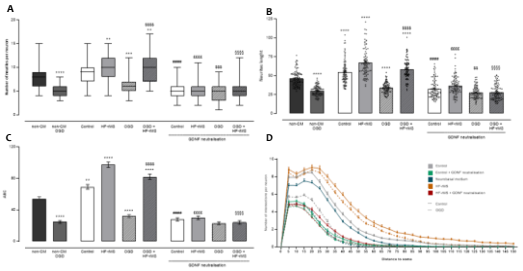

Figure 3. GDNF neutralization hampers the effects of astrocyte-CM on ischemia-induced neurite degeneration. **A.** Number of neurites per neuron. **B.** Neurite length. **C.** Area under the curve from Sholl analysis. **D.** Number of intersections per neuron on the distance to soma determined by Sholl analysis. **P<0.01, ***P<0.001, ****P<0.0001 compared to non-CM; ####P<0.0001 compared to Control; £££££P<0.0001 compared to HF-rMS; $$P<0.01, $$$P<0.001, $$$$P<0.0001 compared to OGD, and §§§§P<0.0001 compared to OGD + HF-rMS.

4. Neutralization of GDNF present in CM from HF-rMS-stimulated astrocytes impedes the effect of this CM on ischemia-induced reduction of c-Fos expressing neurons

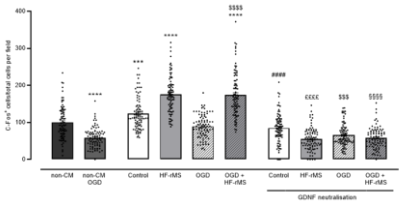

Figure 4. Neutralization of GDNF in CM from HF-rMS-stimulated astrocytes reduces the number of neurons expressing c-Fos. ***P<0.001, ****P<0.0001 compared to non-CM; ####P<0.0001 compared to Control; £££££P<0.0001 compared to HF-rMS; $$$P<0.001, $$$$P<0.0001 compared to OGD, and §§§§P<0.0001 compared to OGD + HF-rMS.

Conclusions

- HF-rMS increases the levels of glutamate transporter EAAT1 in cortical cultures exposed to OGD, suggesting that HF-rMS may decrease the excitotoxicity associated with the ischemic injury.
- GDNF released by HF-rMS-exposed astrocytes contributes to the neuroprotection promoted by HF-rMS in a model of ischemic injury.

References

[1] Radak, D., *et al.* Curr Vasc Pharmacol, 2017. **15**(2): p. 115-122.
[2] Freitas-Silva, M., *et al.* Clin Neurol Neurosurg, 2021. **203**: p. 106564.
[3] Sasaki, N., et al. J Stroke CerebrovascDis, 2013. **22**(4): p. 413-8.
[4] Dionísio, A., et al. J Stroke CerebrovascDis, 2018. **27**(1): p. 1-31.
[5] Chieffo, R., et al. NeurorehabilNeuralRepair, 2014. **28**(3): p. 291-8.
[6] Chieffo, R., et al. Arch PhysMed Rehabil, 2014. **95**(6): p. 1141-7.
[7] Wang, Q., et al. Brain Stimul, 2020. **13**(4): p. 979-986.

FCT COMPETE 2020 PORTUGAL 2020

Certificate of Poster presented at XVII International CICS-UBI Symposium

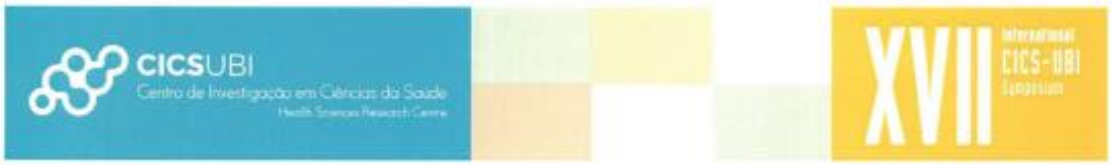

CERTIFICATE

I herewith certify that Susana Ferreira presented a poster in the XVII International CICS-UBI Symposium, which was held the 20th and 21st July 2022.

The Organizing Committee

Certificate of course completion: “V curso para el desempeño de las funciones A, B y C en roedores, lagomorfos, carnívoros, cerdos y pequeños rumiantes”

Centro de Cirugía de Mínima Invasión
Minimally Invasive Surgery Centre
Jesús Usón

Nº ACTA: 26495

CERTIFICADO DE APROVECHAMIENTO

Dª. Susana Maria Alves Ferreira

ha participado como **alumna** en el

“V CURSO PARA EL DESEMPEÑO DE LA FUNCIONES A, B Y C EN ROEDORES, LAGOMORFOS, CARNÍVOROS, CERDOS Y PEQUEÑOS RUMIANTES

Organizado por el Centro de Cirugía de Mínima Invasión *Jesús Usón* de Cáceres.

Celebrado en Cáceres desde el 4 de Noviembre al 17 de Diciembre de 2021.

El Curso ha constado de 103 horas lectivas, incluyendo tanto teoría como práctica sobre las siguientes materias:

- BLOQUE TEMÁTICO I: Legislación Nacional y Europea
- BLOQUE TEMÁTICO II: Ética, bienestar animal y las tres erres (niveles1 y 2)
- BLOQUE TEMÁTICO III: Biología básica de los animales de experimentación. Roedores, lagomorfos, carnívoros, cerdos y pequeños rumiantes (nivel 1).
- BLOQUE TEMÁTICO IV: Cuidados, salud y manejo de los animales. Roedores, lagomorfos, carnívoros, cerdos y pequeños rumiantes.
- BLOQUE TEMÁTICO V: Reconocimiento del dolor, sufrimiento y angustia. Roedores, lagomorfos, carnívoros, cerdos y pequeños rumiantes.
- BLOQUE TEMÁTICO VI: Métodos incruentos de sacrificio. Eutanasia (niveles 1 y 2).
- BLOQUE TEMÁTICO VII: Procedimientos mínimamente invasivos sin anestesia (niveles 1 y 2).
- BLOQUE TEMÁTICO VIII: Anestesia para procedimientos menores. Anestesia avanzada para intervenciones quirúrgicas o procedimientos mayores.
- BLOQUE TEMÁTICO IX: Principios de cirugía.

Dr. Francisco Miguel Sánchez Margallo
Director Científico Centro de Cirugía de Mínima Invasión Jesús Usón Cáceres

D. Luis Dávila Gómez
Jefe del Servicio de Animalario del Centro de Cirugía de Mínima Invasión Jesús Usón. Cáceres

Dña. María Reyes Panadero
Jefa del Servicio de Experimentación Animal de la Universidad de Extremadura

Fundación inscrita en el Registro de Fundaciones del MEC con CIF G 10047417

Ctra. N-521, km. 41,8 • 10071 CÁCERES (SPAIN)
(34) 927 18 10 32 • Fax (34) 927 18 10 33 • email: ccmi@ccmijesususon.com • www.ccmijesususon.com

Certificate of attendance at theoretical sessions of the "Advanced Course on Fluorescence Microscopy and Image Analysis"

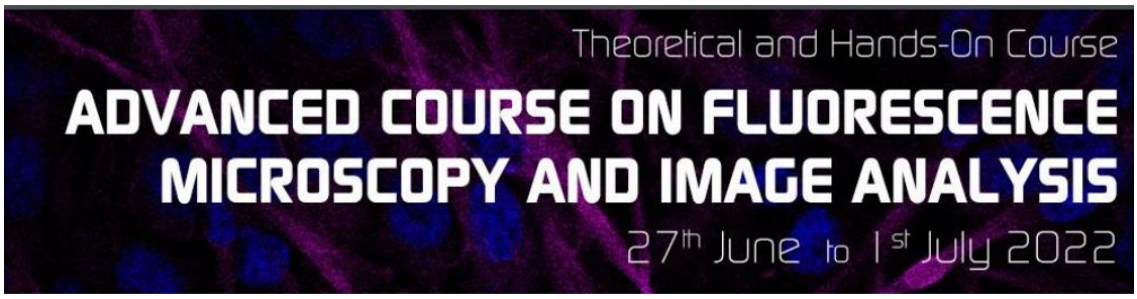

CERTIFICATE OF ATTENDANCE

I herewith certify that Susana Maria Alves Ferreira

has attended the theoretical sessions (15 hours) of the **Advanced Course on Fluorescence Microscopy and Image Analysis**, from the 27th June to 1st July 2022 @ CICS-UBI, Covilhã (Portugal).

The Organizing Committee

Certificate of attendance at XVII International CICS-UBI Symposium

Certificate of attendance at “Webinar de escrita científica – Princípios Gerais para Obter uma Publicação Científica”

Certificado de participação

Certifica-se que

Susana Maria Alves Ferreira

participou no ***Webinar de Escrita Científica***

“Princípios Gerais para Obter uma Publicação Científica”,

realizado no dia 23 de outubro de 2021, com a duração de 6 horas.

ready topub AUTHOR SERVICES PROVIDER

Ricardo Malheiro

Dr. Ricardo Malheiro

Diretor Geral

ReadyToPub – Author Services Provider

#IPSANTARÉM ICEM21 International Council For Educational Media

readytopub.com info@readytopub.com